Review

Viscoelasticity in 3D Cell Culture and Regenerative Medicine: Measurement Techniques and Biological Relevance

Payam Eliahoo, Hesam Setayesh, Tyler Hoffman, Yifan Wu, Song Li, and Jennifer B. Treweek*

Cite This: ACS Mater. Au 2024, 4, 354−384

Read Online

| ACCESS | | Metrics & More | | Article Recommendations |

ABSTRACT: The field of mechanobiology is gaining prominence due to recent findings that show cells sense and respond to the mechanical properties of their environment through a process called mechanotransduction. The mechanical properties of cells, cell organelles, and the extracellular matrix are understood to be viscoelastic. Various technologies have been researched and developed for measuring the viscoelasticity of biological materials, which may provide insight into both the cellular mechanisms and the biological functions of mechanotransduction. Here, we explain the concept of viscoelasticity and introduce the major techniques that have been used to measure the viscoelasticity of various soft materials in different length- and timescale frames. The topology of the material undergoing testing, the geometry of the probe, the magnitude of the exerted stress, and the resulting deformation should be carefully considered to choose a proper technique for each application. Lastly, we discuss several applications of viscoelasticity in 3D cell culture and tissue models for regenerative medicine, including organoids, organ-on-a-chip systems, engineered tissue constructs, and tunable viscoelastic hydrogels for 3D bioprinting and cell-based therapies.

BIOLOGICAL RHEOMETRY TECHNIQUES
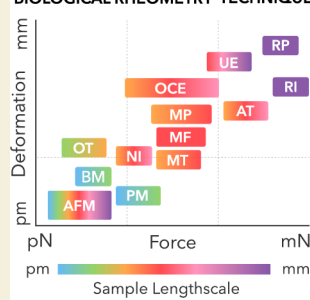
RP: Rotational Plate
AFM: Atomic Force Microscopy
NI: Nano Indentation
RI: Rheolution Instrument
OCE: Optical Coherence Tomography
MF: Microfluidic
MP: Micropipette
BP: Biopolymer
MT: Magnetic Tweezer
OT: Optical Tweezer
AT: Acoustic Tweezer
PM: Passive Micro-Rheology
UE: Ultrasound Elastography

KEYWORDS: *Viscoelasticity, mechanobiology, rheology, elastography, stiffness, mechanical properties, AFM, Nanoindentation, Microrheology, Brillouin Microscopy*

INTRODUCTION

Cells sense their physical environment and respond to chemical, electrical, and mechanical stimuli.[1−3] They probe the mechanics of their environment through mechanotransduction processes that often begin at the level of mechanoreceptor activation, such as through membrane-localized integrin proteins, and proceed via transmission of mechanical stimulus information to the cytoskeleton through changes to the polymerization of actin and myosin. This remodelling of cytoskeleton networks can influence cell behavior through modifying gene expression, with microtubule-actomyosin crosstalk altering nuclear morphology and chromatin accessibility.[4] Reciprocally, biochemical signaling in motor proteins within the cells, such as myosin and F-actin, can activate force generation by cells to influence their environment. The back-and-forth between mechanical and biochemical signals are known as mechanochemical feedback loops,[1] which are understood to regulate cellular processes such as migration, polarization, and fate specification. Additionally, cells exerting forces to their environment require energy and depends on the mechanical properties of the microenvironment which consequently affect cells' metabolism.[5,6] Cell-cycle progression and division, which also require applying force to the microenvironment, are regulated by the mechanics of the microenvironment and contributes to the larger tissue-scale development and homeostasis.[7] Cell−cell communication by gap junction and E-cadherin is also regulated by microenvironment mechanics.[8,9] In development and tissue morphogenesis, the cell size, shape, numbers, position, gene expressions, and metabolism are regulated by biochemical patterning and mechanical forces.[1,10]

Whereas the chemical, molecular, and cellular processes that are triggered by mechanical forces are increasingly well understood for healthy tissues.[1] How these processes differ in the diseased state, and how changes in the mechanical properties of cells and their microenvironments contribute to disease pathology, are areas of growing scientific interest.[11] For example, in epithelial-type cancers as well as fibrosis, the interplay between cells and their microenvironment causes the extracellular matrix (ECM) to stiffen significantly.[12] In the case of epithelial cancers (not fibrosis), cancerous cells that are

transitioning from epithelial to mesenchymal-type will soften, thereby enhancing their ability to migrate and invade surrounding tissues.[13] However, stiffening the ECM negatively impacts the response to chemotherapy[14,15] and thus has been viewed as a druggable target.[16] In addition, recent studies have shown that mechanical forces affect the dynamic and mechanical properties of chromatin.[17] Nucleus response to mechanical forces has been assessed in health and disease states, and the contribution of Lamin and chromatin to mechanical properties of the nucleus has been investigated.[18] Other examples of changes in mechanical properties of ECM that are considered as signs of injury or disease include aging (drooping of facial skin) and wound healing (collagen deposition at the site of injury). Taken together, this evidence suggests that the mechanical properties of the cell, cell organelles, and ECM play multifaceted roles in development, homeostasis, and disease.

Biological tissues form a 3D structure and exhibit the behavior of partially solid and partially liquid materials. Solid materials (e.g., collagen fibers) react to external forces instantaneously, whereas liquid (e.g., water) and fluid (e.g., plasma) respond in a time-dependent fashion. Fluid deformation (displacement) is not reversible when the stress is removed. If the stress on solids is small enough that it does not cause permanent (plastic) deformation or a fracture, they demonstrate an elastic response, recovering to their original state after removal of the stress. The time-dependent behavior of liquid materials to external stress is called viscosity.[19] In the ECM, macromolecules such as collagen and elastin, generally behave like solids and contribute to the elastic response of the ECM. But, any rearrangement of these macromolecules also takes some time, so while they contribute to the viscosity of the ECM to some degree, their contribution is not as significant as that of liquid within the ECM. Other molecules within the ECM, such as hyaluronic acid, attract water, which contributes to its viscous response.[20] In a cell, filaments such as actin, myosin, and microtubules contribute to its elastic response, while the cell-filling cytoplasm contributes to its viscous behavior.[2] Due to this solid–liquid-like behavior of biological tissues, which mediates their dual elastic and viscous responses to applied stress, they are considered viscoelastic materials. It is worthwhile to note that other behaviors such as plasticity and nonlinear elasticity from high levels of stress, as well as poroelasticity due to the porosity of tissue, also impact the behavior of biological tissues to mechanical forces, but these topics our outside the scope of this review.

ECM viscoelasticity and cell mechanotransduction play critical roles in tissue development, wound healing, aging, and diseases such as cancer and fibrosis. Thus, efforts to better understand and model the viscoelasticity of the tissue microenvironment and the mechanisms of mechanotransduction health and disease could lead to new methods for disease treatment, called mechanotherapy.[21] Here, we provide an overview of basic concepts in the field of linear viscoelasticity and then discuss various measurement techniques that are commercially available or under development. Lastly, we summarize how these viscoelasticity measurement technologies could benefit research within the fields of regenerative medicine and tissue engineering.

1. VISCOELASTICITY

1.1. Key Concepts

External forces on a body of material (solid, liquid, or a mixture of the two) result in either movement of the body as a whole or motion in some particles called deformation. Deformation can be reversible (elastic as observed for solid materials) or irreversible (viscous, flow, plastic, or fracture), as depicted in Figure 1. Plastic deformation and fracture are
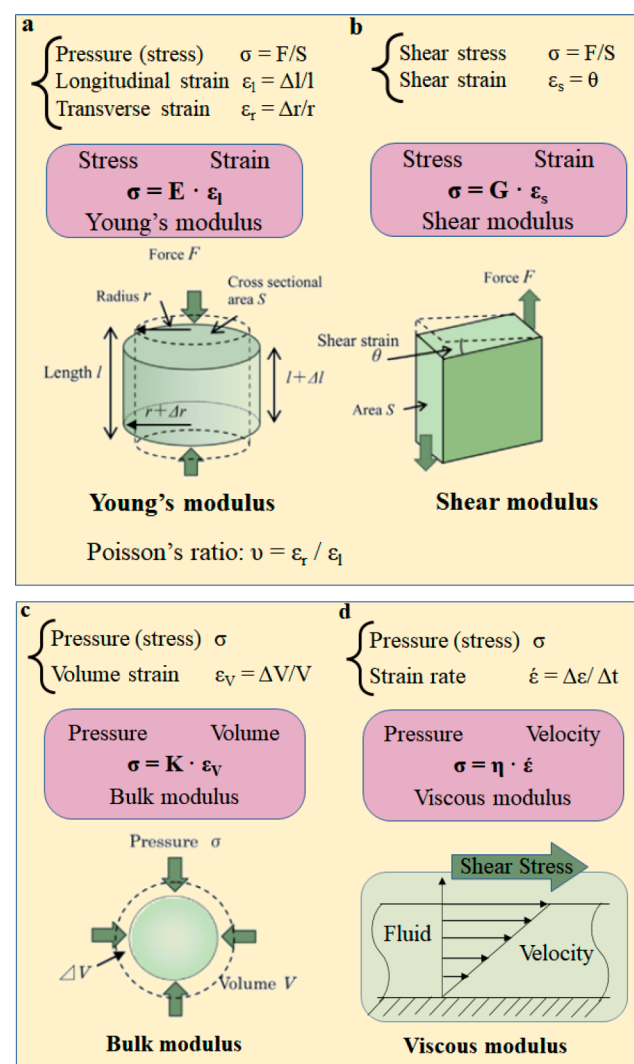
Figure 1. (a) Axial force causes elongation or compression in the direction of force and inverse deformation on the perpendicular direction of force (Poisson's ratio). (b) Tangential (shear) force causes shear deformation. (c) Volumetric pressure results in bulk deformation. (d) Shear stress on fluid causes flow of the material.

observed in solids. Viscous deformation and flow of the material are observed in liquids. In the field of rheology, a material's behavior is described in the form of constitutive equations that specify the properties of material which depend only on its nature, not on its of size or shape. When a material is subjected to an input of energy, a portion of this energy is stored, and the rest is dissipated. This is a simple consequence of the second law of thermodynamics. Because the dissipation never occurs instantaneously, the material properties are known to be time-dependent. Dissipation occurs via viscous mechanisms (flow); therefore, a material's displacement

(deformation) lags the excitation force. The length of the lag or delay depends on the duration of the excitation force. For example, if the excitation time is very short, material molecules do not have sufficient time to rearrange. If the excitation is very long, then there is sufficient time for molecules to rearrange. Almost all biological materials show both elastic and viscous properties and, therefore, they are classified as a viscoelastic material. If the applied stress is small enough, the material will behaves within a region called linear viscoelasticity or linear time-dependent. However, when the input energy is high, the material's behavior will become nonlinear.

The most important feature of viscoelastic behavior is the time dependency property of the material. Applied stress on the material rearranges particles inside the material, and for any real material, a finite time is required for the rearrangements. When rearrangement occurs very quickly, the material is regarded as purely viscous, and all of the energy required to cause the deformation is dissipated as heat. When the material rearrangement takes a very long time, it is regarded as a purely elastic material, in which case the energy is stored and can be recovered after releasing the force. Water is considered to be close to a purely viscous material, while steel behaves almost like a purely elastic material. In a typical viscoelastic material, the rearrangement time is comparable with the time of applied stress (also referred to as experiment). For a time-dependent material, the relation between shear stress and shear strain is given by

$$\sigma(t) = G(t)\varepsilon$$

where $\sigma(t)$ is the time-dependent stress, ε is the deformation, and $G(t)$ is called the shear modulus or relaxation modulus.

Another form of describing the stress−strain relationship is by

$$\varepsilon(t) = J(t)\sigma$$

where $J(t)$ is creep compliance. $J(t)$ and $G(t)$ are not the inverse of each other, because material responds differently in time with stress excitation or strain excitation. The relation between $G(t)$ and $J(t)$ is given by

$$G(t)J(t) \leq 1$$

and the equal sign is valid only when time is infinitely short or infinitely long.

Applying a tensile force or compression force in the axis of the rod causes deformation in the form of extension or elongation, which is the simplest form of deformation. For a Hookean solid or purely elastic material, the relationship between stress and strain is linear. E is a constant known as the Young's modulus or elastic modulus and is often called stiffness. The constitutive equation is written as

$$E = \sigma/\varepsilon_l$$

where σ is the stress and ε is the strain. If the force is exerted tangentially on the material, then it can cause a different form of deformation. This force is called shear force, and shear stress is defined by the tangential force over the surface area. The shear strain is defined by a change in radians. The shear modulus is defined as

$$G = \sigma/\varepsilon_s$$

For materials that are homogeneous and isotropic, the shear modulus and Young's modulus are related by

$$G = E/(1 + v)$$

v is called Poisson's ratio and is the ratio of lateral contraction to the elongation in the infinitesimally small uniaxial extension. For compressible materials, applying force volumetrically from every angle causes shrinkage or change in the volume, and the relationship between stress and strain is defined by bulk modulus. Most materials, including all liquids, are incompressible. If the liquid is contained between two parallel plates and one plate moves at a constant velocity, at the steady state situation, liquid velocity establishes a gradient depending on the separation of plates. The constitutive equation is written as

$$\eta = \sigma/\varepsilon$$

The coefficient of shear viscosity (η) or viscosity in short is a material property independent of its form and shape. The liquid materials obeying this constitutive equation are called Newtonian Fluids.

When designing a new biomaterial such as hydrogels for 3D bioprinting or for cell therapies that need a hydrogel as a delivery mechanism, the elastic and viscous moduli as well as Poisson's ratio need to be tuned closely to the host tissue for optimal biomimicry. Another example of tuning viscoelasticity of the ECM is organs-on-a-chip for understanding and modeling the disease. By tuning the viscoelasticity of the organoid ECM close to the in vivo case, the model can recapitulate the disease progression and response to the therapy closer to the in vivo case and provide a more accurate model and eventually a better clinical outcome.

1.2. The Creep and Relaxation Measurements (Experiments)

In rheology, the material of interest is under known stress, and the strain is measured over time or vice versa. It is important to note the difference between the viscoelasticity and the plasticity of a material. A deformed plastic material will not return to its original shape and form after stress is removed, but a viscoelastic material will return to its original shape after the deforming force is removed if the deformation is small enough and the material is probed within its linear viscoelasticity region. Some materials might show a combination of elasticity and plasticity. They partly return to the origin, and some permanent deformation remains in the material after removal of the stress load. Figure 2a depicts various materials' behavior under stress conditions. In this review, we focus on viscoelastic materials. The experiments performed on viscoelastic materials are categorized to two major types: transient and dynamic. In the transient experiment, a sudden deformation is applied to the material, and its response is observed over time. The dynamic experiment is the one in which either stress or strain is varied cyclically over time, and the response is observed at a range of frequencies of deformation. In practice, transient experiments are easier to perform and to understand. The transient experiments can be done in two ways. One is to load the material with sudden stress and observe the deformation over time. It is called the Creep test. Figure 2b shows how the strain changes over time with constant stress. Compliance is defined by strain over stress which is approximately inverse of stiffness. The second type of transient experiment is called the stress relaxation experiment. In this test, a material goes under sudden deformation (controlled strain), and the stress that is required to sustain the deformation is measured over the time. Due to viscoelastic properties of the material, the stress required to keep the material at a constant deformation fades
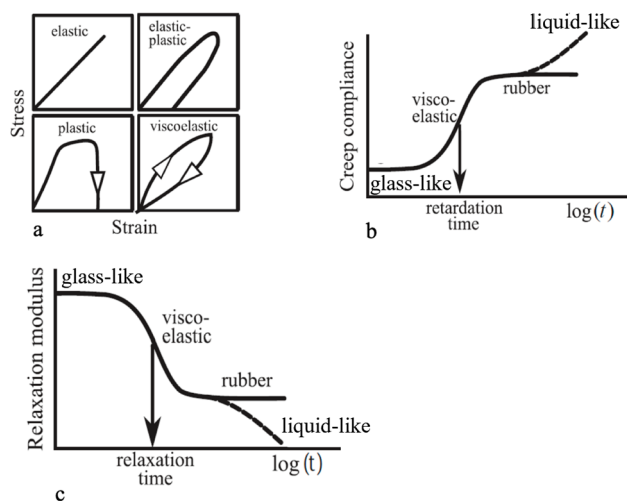
Figure 2. (a) Relationship between the stress and strain in elastic, plastic, elastic-plastic, and viscoelastic material. (b) Creep test over time for various materials. (c) Relaxation test over time for different material types.

Figure 3. (top) Purely elastic materials show no phase difference between stress and strain. (middle) Viscoelastic materials show phase difference between the stress and strain signal. (bottom) Shear modulus in viscoelastic materials is a vector summation of two orthogonal components, storage (elastic) modulus and loss (viscous) modulus.

away; this is referred to as relaxation. Figure 2c shows how the stress changes over time with a constant stain.

1.3. The Dynamic Response

Both stress-relaxation and creep tests can be executed easily, and the measurement data can be simply interpreted. However, dynamic testing can offer much more insights into the material behavior over a wide range of stress/strain rates even if the geometry of the material is rigged. Dynamic testing especially is suited for biological materials that are nonlinear in nature, but if the deformation is small enough, they can be considered linear in that region. In dynamic testing, the material is subjected to stress or strain sinusoidally at varying excitation. If the material is purely elastic, the stress and strain functions will have no delay or lag with respect to each other as shown in Figure 3-top.

For a purely viscous material, the sinusoidal strain is proportional to the variation of accelerations in strain, which results in the stress lagging the strain by 90°. For a viscoelastic material, the response is partly elastic and partly viscous. Therefore, the response to sine excitation would lag between 0° and 90°. If the modulus is measured at the highest strain, it is defined as the storage or elastic (real) modulus. If the modulus is measured at the highest strain rate, it is defined as loss or viscous (imaginary) modulus. When G' is the storage or elastic modulus and G'' is the loss or viscous modulus, the shear modulus representing storage and loss moduli and the phase difference δ are computed as follows:

$$G(\omega) = G'(\omega) + jG''(\omega)$$

$$|G(\omega)| = \sqrt{G'(\omega)^2 + G''(\omega)^2}$$

$$\tan \delta = \frac{G''(\omega)}{G'(\omega)}$$

2. RELEVANCE OF VISCOELASTICITY IN BIOLOGY

Forces exerted on cells are sensed by either protein-based mechanosensors or cytoskeletal- and nuclear-deformation-mediated molecular responses. These external mechanical
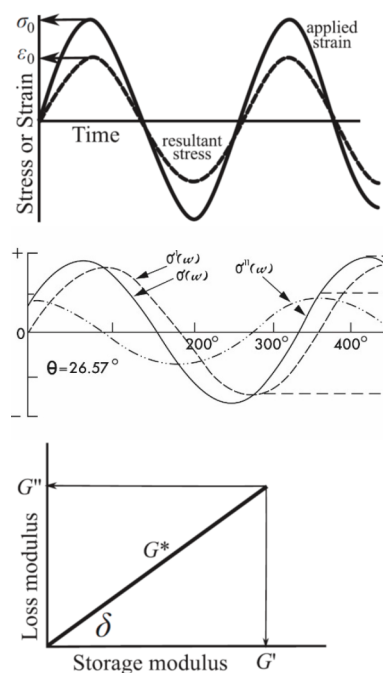
cues are translated into biological signals that can be transmitted from the membrane to the cytoplasm and nucleus in a process called mechanotransduction. For example, in the cell-matrix interface, focal adhesions on the membrane convert mechanical information in the ECM to biological activities and propagate the signals to the nuclear membrane through cytoskeletal filaments.[22] Linker of nucleoskeleton and cytoskeleton (LINC) complexes form a bridge between the cytoplasm and nucleus, and which can help to convey mechanical signals to the nuclear lamina and associated chromatin in the nucleus,[23] and thereby influence gene expression.[17−27] These ideas are summarized in Figure 4, which depicts the cascading effects of ECM viscoelasticity on cellular and gene regulatory processes.

With the understanding that living tissues and the ECM exhibit more complex mechanical properties such as viscoelasticity rather than linear elasticity, it follows that cell and ECM viscoelasticity causes the applied forces to partially store and partially relax within the cells or tissue, which in turn elicits a shifting pattern of biochemical responses to these forces.[24] Recent years have witnessed efforts to decipher the influence of matrix viscoelasticity on diverse biological processes including embryogenesis, tissue development, tissue function, homeostasis, disease progression, response to therapy, and cell metabolism.[25−35] Here, we briefly review some of the ways in which tissue viscoelasticity, and the corresponding cell-ECM interactions, regulate cell and tissue behaviors during normal development as well as in disease progression.

2.1. Viscoelasticity of Cell and Cell Organelles

Cells comprise a bilipid membrane (flexible), cytosol (fluid), nucleus, and the organelles in the cytoplasm. The three major
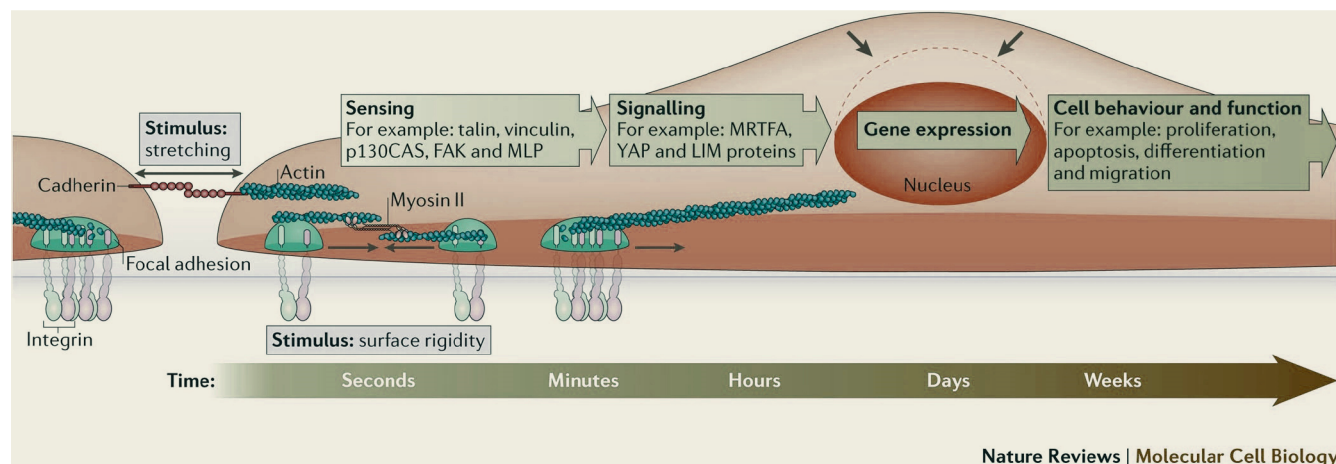
Figure 4. The process of mechanotransduction translates the microenvironment viscoelasticity and cell–cell tension forces into chemical signals to regulate the cell processes. Typically, integrin proteins form the focal adhesion between the cell and ECM. Cadherin proteins are responsible for cell–cell forces. Focal adhesion is regulated by environment viscoelasticity and through polymerization of actin and myosin; the mechanical cues are transmitted to the nucleus and result in change of gene and protein expressions. Focal adhesion kinase (FAK); muscle LIM protein (MLP); myocardin-related transcription factor A (MRTFA); yes-associated protein (YAP). Adapted with permission from reference 24. Copyright 2014 Nature Publishing Group.

biopolymers within the cytoskeleton are actin filaments, microtubules, and intermediate filaments.[36] These flexible filaments are sufficiently rigid to provide mechanical support for the cell, and together with the nucleus, these filaments, each of differing rigidity, form the major determinants of a cell's elastic character. A cell's viscous property stems from the cytosol, which is the fluid confined within the flexible membrane.[24] Under stress, water molecules of the cytosol move within the membrane and dissipate the exerted energy on the cell, which determines the viscous component of the cell. The filaments resist deformation, and when stress is removed, they will restore the cell to its original shape. It is important to note that the filaments in the cytoskeletons are not static. They are nonlinear and flexible structures.[36] In addition to forming a scaffold for the cell, they provide pathways for motor proteins to move and attach the membrane to the rest of the cell. Their assembly is spatially organized within the cytoskeleton.[37] The nonlinearity of the filaments is especially important under conditions where a large magnitude of stress is exerted upon the cell, filaments display higher rigidity (elastic modulus) to limit their deformation. In helping to maintain cell shape, this nonlinearity plays a protective mechanism. Filament entanglement through branching, cross-linking, and bundling forms a heterogeneous network in which the pattern of linkages between filaments and the geometry of their arrangement give rise to the cell's elasticity.[37] Although the surface charge density of filamentous networks does not affect the elasticity of filaments, the status of these biopolymers as highly charged anionic polyelectrolytes comes into play as filaments bind to proteins and form the geometry of the network, which shapes contributes to the overall elasticity of the cell.[37]

The nucleus is the largest and stiffest organelle in eukaryotic cells, and the elucidation of the molecular pathways that transmit mechanical forces from the cell membrane to the nucleus is under active study. Much evidence suggests that the sensing of external forces by integrin receptors on the cell membrane leads to nuclear deformation and chromatin reorganization.[37] Nesprin and SUN proteins form an important structural link between the nucleoskeleton and

cytoskeleton. On the inner nucleus membrane, the SUN proteins are connected to the nuclear lamina that affect chromatin rheology and eventually gene expressions.[37] Figure 5 illustrates the force transmission from the cytoskeleton to the nuclear lamina.
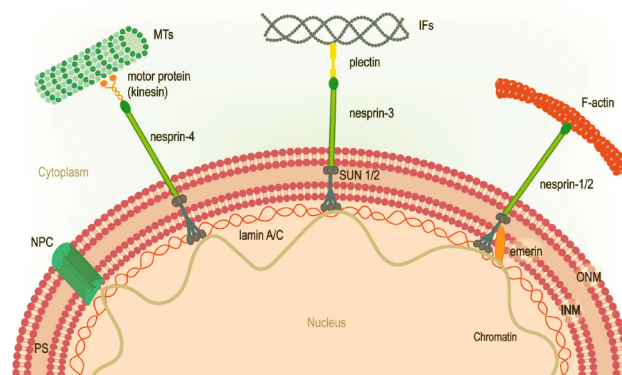
Figure 5. Nucleus and cytoskeleton connection. Outside the outer nuclear membrane (ONM), different nesprin isoforms connect to F-actin, intermediate filaments (IF), and microtubules (MTs). SUN proteins bind to nesprins in the perinuclear space (PS) and interact with nuclear lamina through lamin A in the inner nuclear membrane (INM). Emerin proteins connect the Sun proteins to lamin A and directly interact with chromatin. Adapted with permission under a Creative Commons [CC-BY 4.0] from reference 37. Copyright 2018 Frontiers Media.

Rheological studies on lamins and chromatin have reported that lamin-A and lamin-B1 contribute to the elastic modulus of the nucleus, while its viscous modulus mostly stems from lamin-A and nucleoplasm.[18] The viscosity of nucleoplasm impacts the rates of molecular transport inside the nucleus.[17] Viscoelasticity of the nucleus plays an important role in the cell epigenetic state and cell reprogramming. A recent experiment has shown that a rapid (millisecond) nuclear deformation through a microfluidic channel caused a boost in conversion of fibroblasts into neurons at the early stage of cell reprogramming.[38]

Less is known about the effect of cell and ECM viscoelasticity on the behavior and function of other cell organelles, and vice versa. A recent study demonstrated that membrane ruffling acts as a mechanosensor of ECM viscosity that regulates single-cell motility, focal adhesions, and forces generated by the cell.[39] The reciprocal connection between viscoelasticity and cell metabolism is another area of interest, whereby tissue mechanics may help to pattern cell nutrient utilization and mitochondrial shape mitochondrial shape, as part of a control mechanism for energy generation and biosynthesis of macromolecules.[40]

2.2. Viscoelasticity of ECM and its Main Contributors

The emerging field of mapping both elastic and viscous moduli of the ECM is gaining prominence. The viscous modulus of tissue microstructure represents a promising novel biomarker for disease, and hence the longitudinal tracking of tissue viscoelasticity in patients could revolutionize diagnostic medicine. For example, pathologies such as tumors and fibrosis are characterized by consistent changes in the structural properties of these anomalies, with a stiffer segment appearing within tissue. While histological examination can reveal this microstructural change, repeated measurements of tissue viscoelasticity in a noninvasive fashion could document these biological changes over time, which might in turn inform uncovering possible targets for therapeutic intervention.

At the microscale, the two main components of tissue are the ECM and active cells, such as fibroblasts and smooth muscle cells. As mentioned above, cells residing in the tissue are viscoelastic. Cells display changes in their viscoelastic properties when they progress to malignancy. For example, malignantly transformed fibroblasts have a reduced loss modulus compared to normal fibroblasts.[41] Accordingly, developing techniques to monitor the changes in cells' and tissue's viscoelastic properties has great potential to help the early identification of disease progression. In this section, we will focus on the other component of the tissue micro-structure—ECM.

During development, the ECM undergoes continuous remodeling to maintain tissue homeostasis, which includes not only the homeostasis of biochemical molecules but also mechanical homeostasis related to tissue-level structural integrity and functionality.[42] To illustrate this point, Figure 6 highlights the remodeling of the cervical ECM during pregnancy. The mechanical properties of the ECM mainly depend on fibrillar collagens, elastic fibers that consist of elastin and microfibrils, glycosaminoglycans (GAGs), and the related proteoglycans (PGs), with each of these ECM components subserving a load-bearing role.

Providing structural support to the ECM, fibrillar collagen counteracts tissue deformation when there is mechanical loading. Herein, the density, orientation, and cross-linking of collagen fibers within the ECM change dynamically in response to the forces experienced by the tissue environment.

Elastic fibers contribute to the elasticity of ECM. Elastin fibers are pre-stressed during their formation and upon their assembly. They stretch to discharge the stress, which causes them to curl around the attached collagen fibers, while collagen fibers contract during stress. Operating like springs, elastin fibers support the collagen fibers by recoiling. They withstand repeated loading cycles and have linear responses up to 100% strain with an average stiffness of 0.4 MPa (approximately 2 orders of magnitude lower than collagen). Mechanical damage or abnormal proteolytic degradation of these fibers leads to irreversible changes in tissue structure and functionality, resulting in the transition of tissue from a healthy to diseased state.[43]

Glycosaminoglycans (GAGs) and the related proteoglycans (PGs) also contribute to the viscous properties of the ECM by filling in the space between the fibers in an orthogonal, scattered network. They provide support for the bending action of collagen. GAGs and the attached PGs attract water and generate an osmotic pressure, thereby operating like a dashpot or dampener against compression and relaxing stress on the ECM.[20]

The overall architecture of the ECM, which is comprised of a naturally formed interpenetrating polymer network of fibers and glycans, also endows viscoelasticity. Soft tissues including breast, liver, skin, muscle, and adipose substantially relax over the stress in a time scale of 10 to 100 s. Even skeletal tissues such as bone, cartilage, tendons, and ligaments are viscoelastic. Rheological data, including dynamic response and stress relaxation tests, show that biological tissues exhibit viscoelastic response with a viscous modulus of about 10−20% of the storage modulus. The viscoelasticity of ECM and tissue has also been observed to be highly variable (the loss modulus of different tissues was measured from several to billion Pascals),[44] which suggests the important role of matrix viscoelasticity on the regulation of cell behaviors.

2.3. Viscoelasticity as a Biomarker for Cell−ECM Interactions

There exists a reciprocal crosstalk between cells and their matrices.[40,45] While cells sense the mechanical changes of ECM and respond through the formation of nascent integrin adhesions and reorganization of cytoskeletal filaments,[46] the macromolecules in ECM also assemble/reassemble according to the secretion of biochemical signals from cells. The disruption of cell−ECM interactions is recognized as a key factor in diverse pathologies including fibrosis, osteogenesis imperfecta, and even carcinomas.[43] Therefore, understanding the interplay between cells and ECM is critical to help the early diagnosis of diseases and to provide possible solutions for disease treatments. Since cells and ECM are both viscoelastic and the viscoelastic properties differ in healthy and abnormal cells and tissue, it is of prominent importance to elucidate the

▨ Collagen fiber	▬ PGs	🌿 Epithelium
▭ Elastin fiber	— Basement membrane	• Fibroblast
▬ Hyaluronic acid	⊚ Matricellular protein	▨ Muscle cell
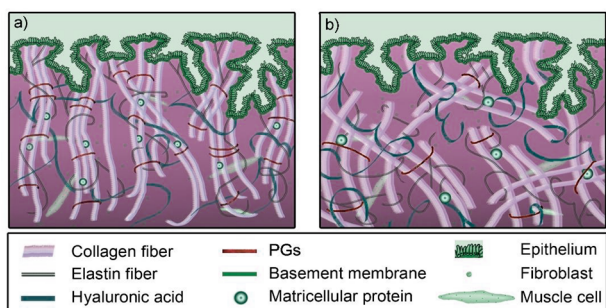
Figure 6. Remodeling of the cervical ECM during pregnancy. (a) The architecture of ECM components in nonpregnant women. (b) The morphological changes near the end of pregnancy. Water contents increased, the diameter of collagen fibers increased, crimping increased, and PGs are loosened in (b). Adapted with permission under a Creative Commons [CC-BY 4.0] from reference 20. Copyright 2020 Sensors.

role of viscoelasticity on cell−ECM interactions to uncover the mechanisms for disease prevention and detection.

In recent years, it has been established that matrix stiffness regulates fundamental cell behaviors, such as cell morphology, metabolism, migration, proliferation, and differentiation of diverse cell types.[40,47−52] Recent studies have highlighted the role of matrix physical properties that, through intracellular processing, influence specific pathways of cell metabolism. Healthy cells typically modulate glycolysis based on surrounding mechanical properties, and in the case of lung epithelial cells, reduce activity on softer substrates.[5] Other works demonstrate that softer substrates can increase lipid synthesis.[6] Substrate mechanical properties can also directly influence cell−cell interactions,[9] via changes in gap junction formation, or chromatin accessibility by modulating actomyosin assembly.[4]

Environmental mechanical properties can directly influence the cell phenotype and disease-state. By developing measurement techniques for profiling the physical parameters of different tissues, and then engineering strategies for tuning the mechanical properties of biomaterials to that of healthy or diseased tissue, researchers can translate the field of tissue biomechanics from basic science into clinical medicine. For example, AFM measurement of the stiffness of human brains at different ages revealed the role of niche stiffness on the aging of central nervous system progenitor cells, a finding which holds implications into the diagnosis of neurodegenerative disorders.[53] The construction of three-dimensional (3D) hydrogels, whose mechanical properties better mimicked those of hematopoietic tissues, enabled studies on how matrix stiffness regulates the proliferation of some acute myeloid leukemia types in a biphasic manner by autocrine regulation, knowledge that has relevance in cancer treatment.[54]

Nevertheless, the plethora of roles that viscoelasticity can play across different biological systems remains poorly understood. The development of tools for measuring the viscoelastic properties of materials will empower researchers to investigate the unique function of viscoelasticity in modifying cellular processes. Matrix viscoelasticity has been shown to influence cell geometry, migration, differentiation, spheroid and organoid morphogenesis, cartilage matrix formation, and vascular morphogenesis.[55−60] Likewise, matrix viscoelasticity may precipitate the transition alteration between normal and abnormal tissue to unravel the contribution of the matrix viscoelasticity on disease development. For example, a microrheology-based force spectrum analysis (FSA) technique has been developed to identify the active and passive fluctuations of the ECM in 3D cell culture models, which demonstrated simultaneous cell-mediated matrix stiffening and fluidization causing breast cancer invasion.[61] However, mechanotransduction pathway studies are needed to understand how cells sense viscoelasticity and distinguish it from other physical properties of the ECM, which significantly depends on the development of viscoelasticity measurement techniques.[50]

3. VISCOELASTICITY MEASUREMENT TECHNIQUES FOR IN VITRO AND EX VIVO MODELS

The magnitude of forces that exist between cell−ECM and cell−cell span from pico-Newtons to near micro-Newtons, and the time of their interactions can span from milliseconds to weeks. Therefore, viscoelasticity measurements of biological tissues may range from a few Pascals (e.g., fibrin) to giga-

Pascals (e.g., bone) across a time scale of a few milliseconds to hours.[44] A single instrument cannot capture this broad range of stress and time scales. Consequently, many different instruments for assaying viscoelasticity of biological samples have been designed, and a subset of these have been commercialized. The more prominent techniques that have gained traction in industry and research laboratories are highlighted below; before selecting an approach for accurately and precisely measuring viscoelasticity, the researcher must consider how the sample geometry and size, boundary conditions, the nature of the material and of the supporting material (e.g., glass slide, hydrogel matrix, plastic cell culture dish, etc.), and the overall experimental workflow (e.g., number of samples to be measured, frequency of measurement, time constraints of the assay, etc.).

3.1. Rotational Rheometer

Rotational rheometers are the most used class of instruments to measure the viscoelasticity of a soft material. The sample is sandwiched between a rotary plate and a stationary plate, and the shear stress generated by the relative movement of these two plates causes the sample to deform. Two basic schemes are used in controlling the rotary axes:

(1) Controlled Stress input and measuring the resulting shear rate or CS-rheometers.
(2) Controlled Shear Rate input and measuring the resulting shear stress or CSR-rheometers.

A representation of the above two methods is illustrated in Figure 7.
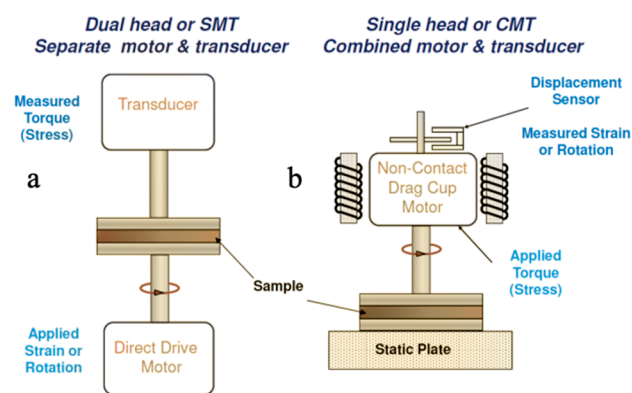
Figure 7. (a) Controlled Shear Rate system diagram. (b) Controlled Shear Stress system diagram.

Some modern equipment can operate under both schemes, but generally, they are optimized for one mode. In addition to measuring either the shear stress or shear rate, in both modes, the phase difference between the shear stress and shear rate in the dynamic test is measured, which indicates how slow or fast the material responds to the external mechanical stimuli. The viscosity is not directly measured by rheometers, but instead, it is deduced from the interdependency of the shear rate and shear stress. The Controlled Stress rheometers are designed to provide high sensitivity at very low values of shear rate, for which simple viscometers cannot provide accurate data. In non-Newtonian fluids such as x and y, the increase in shear rate does not lead proportionally to an increase in shear stress, as is the case for Newtonian fluids such as a and b. Therefore, for non-Newtonian fluids, the Controlled Shear Rate rheometers offer better sensitivity. For very soft solid materials that show

elastic and viscous behavior as a function of shear rate and shear history, the Controlled Stress rheometers outperform the Controlled Shear Rate rheometers. In short, the Controlled Stress rheometers are especially designed to determine the viscoelastic properties of fluids and soft solid materials. The samples are subjected to a small strain oscillation amplitude in a dynamic test and small strain in a creep test.

Various geometries of material holders are offered by the manufacturers, and special attention to the size and shape of these geometries should be paid according to the viscosity of the sample before choosing one. These geometry options include:

(1) Concentric Cylinders; for very low to medium viscosity fluids
(2) Cone and Plate; for very low to high viscosity fluids
(3) Parallel Plate; for very low viscosity to soft solid materials.
(4) Torsion Rectangular; for solids

Figure 8 highlights some geometries for the rotational plates, and Figure 9 depicts a variety of plate sizes.

Figure 8. Geometries are available for rotational rheometers.

Figure 9. A variety of sizes of cones and plates are available. The larger sizes are recommended for low viscosity materials, and smaller sizes are recommended for high viscosity materials.

Based on the viscosity of the material, the proper geometry of either the cone or cylinder should be considered. If the viscosity is very low and the material is very fluid, concentric cylinders are preferred. Cone and plate are used for low viscosity fluids. Parallel plate is mostly used for soft materials such as gels and hydrogels. For solid materials, a rectangular torsion is recommended to measure Young's modulus.

The concentric cylinders are used for very low viscosity fluids, weakly structured samples, and high shear rate measurements. Various shapes of cups and rotors are available to cover a wide range of fluids. The parallel plate geometry is mostly used for soft gels, low to high viscosity fluids, materials with large particles, and samples with a long relaxation time. Temperature ramps and sweeps are available if the material's properties need to be measured over a range of temperatures. The parallel plate requires a good grasp of the material at the top surface to accurately measure the shear rate. For very soft materials where the top plate might slip, crosshatched and sandblasted plates should be considered to avoid slippage. Larger diameter plates apply higher shear stress than smaller plates. The gap between two plates should be carefully considered, because by reducing the gap, the shear rate increases. Effective shear rate varies across a parallel plate because the distance from the center to the edge varies. Therefore, for any given angle of deformation, there is a greater arc of deformation on the section of the material that is located near the edge versus the center of the plate. For solid materials, rectangular and cylindrical torsions are used to measure elastic and viscous moduli and compute the phase difference between them. Also, DMA bending and tension are available to measure Young's modulus.[62,63]

On the parallel plate, the cone plate applies a constant shear rate on the sample as depicted in Figure 10. The distance
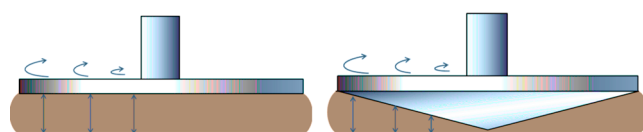
Figure 10. Parallel plate vs cone plate. The cone plate applies constant shear rate.

between the apex of the cone to the plate is called truncation or gap. Cone plate is used for fluids with very low viscosity, high shear rate, and unfilled samples. The cones come in different diameters and different angles. By decreasing the diameter of the cone, the shear stress increases, and by reducing the angle of the cone, the shear rate increases. The gap should be at least ten times bigger than the particle size in the material.

3.2. Atomic Force Microscopy

In 1986, the IBM scientists who had developed the scanning tunneling microscope introduced the Atomic Force Microscope (AFM). AFM uses the mechanical force between the tip and the surface of the sample to generate an atomic resolution image of the material. This technique can be applied to any material in ambient atmospheric pressure and even in aqueous environments, and it can achieve a spatial resolution of 0.01 nm and a force resolution of pico-Newtons. This spatial resolution translates to 300 million times magnification. The AFM system consists of an atomic-scale sharp probe attached to one end of a microcantilever. The cantilever length is in the range of several micrometers. The other side of the microcantilever is connected to a dither piezo actuator that brings the cantilever and consequently the tip of the probe very close to the surface of the sample. Such proximity of the tip to the sample creates either a very weak retention or repulsive force between the tip and sample. The magnitude of this force changes the deflection of the cantilever. A laser beam impinges upon the top end of the cantilever, and its reflection is detected by a photodiode. The photodiode is designed for a quadrant position-sensitive geometry that can detect normal and torsional cantilever deflection simultaneously. The force exerted on the surface of material is proportional to the angle of deflection of the cantilever, which translates to a change in the angle of reflection of the laser beam as illustrated in Figure 11. The sample is placed on a piezoelectric positioner to scan the surface of the sample, and that is how the
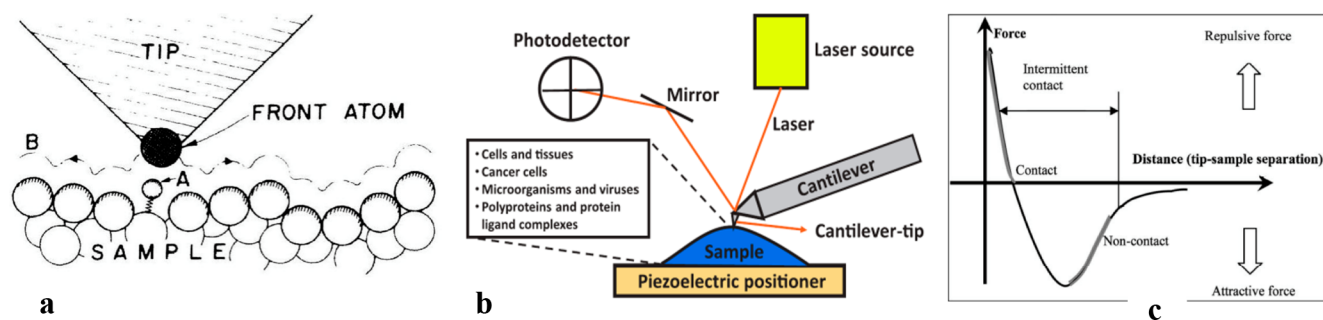
Figure 11. (a) The first drawing of the AFM tip in the vicinity of the sample. (b) Basic system diagram of AFM. By moving the cantilever on the sample surface, the angle of laser reflection from the cantilever changes, which the photodetector records. (c) Information obtained by AFM is in the form of a force–distance curve. Each pixel requires at least one force–distance plot to obtain material property at that point. Adapted with permission from references 64 (Copyright 2003 The American Physical Society) and 65 (Copyright 2021 Portland Press).
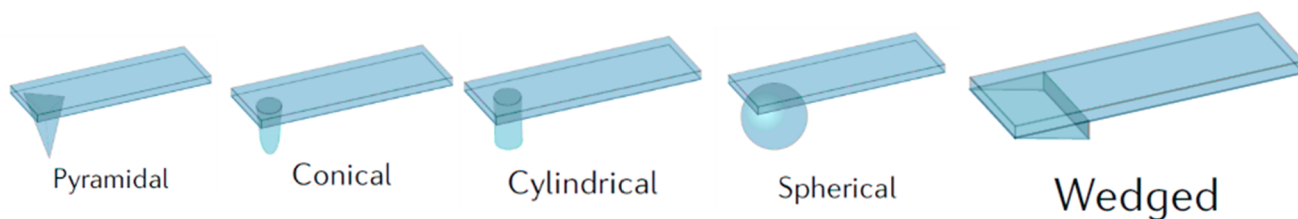
Figure 12. A variety of cantilever tips are available for different material types and stiffnesses. Pyramidal tip shape is mainly used for solids. For softer material, other shapes of the tip should be considered. Each tip has its own computational model to extract the material properties accurately. Adapted with permission from reference 66. Copyright 2019 Springer Nature.
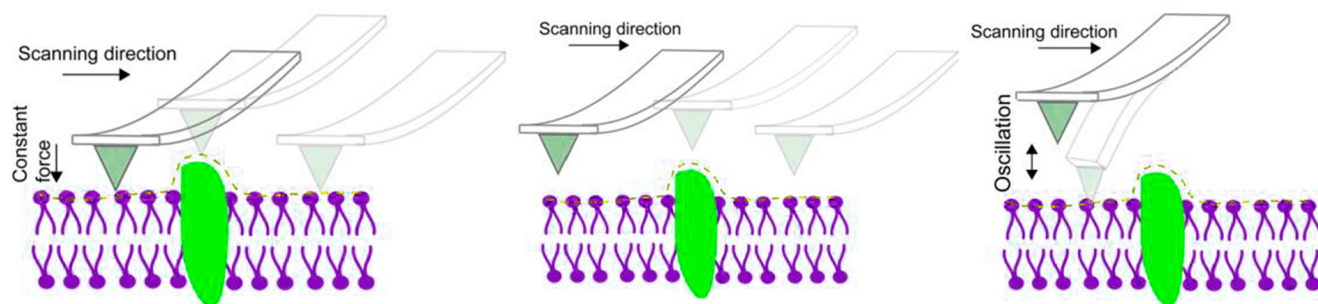
Figure 13. AFM operates in 3 distinct modes. In contact mode (left), the tip of the cantilever touches the surface of the material and scans it. In the noncontact mode (middle), the tip hovers above the surface of the material and oscillates at a very small amplitude. The retention and repulsive forces between the tip and the material of interest cause deflection on the cantilever, which changes the amplitude or the frequency of oscillation. In the semicontact mode (right), while the tip oscillates above the surface of the sample, occasionally touches the material to eliminate the effect of material adhesion and friction. Adapted with permission under a Creative Commons [CC-BY 4.0] from reference 67. Copyright 2018 BioMed Central.

topography of the sample in the X–Y-plane is imaged. The AFM scanner can move in the Z-direction; however, that movement is limited to a few micrometers. The force–distance curves measured by AFM quantify the forces between the tip and the sample and the mechanical response of the sample under the loading condition. For properties that are time-dependent such as the viscous modulus of the sample, force is plotted over time in force–time curves. To address the heterogeneity of the sample or mapping the mechanical properties or morphology of the sample, at least one force–distance curve or force–time curve is recorded per pixel of the image that is measured by AFM topography.

The principle of detecting the mechanical properties of the sample is based on the forces between atoms of the tip and the sample. When the tip is too far from the sample, the forces are attractive, and when the tip is very close to the sample, they are repulsive.

Modes of Operation. There are three modes of operation of AFM: 1) contact mode, 2) noncontact mode, and 3) semicontact mode. 1) In the contact mode, the tip is in direct and slight contact with the sample, and the scanner maintains a constant force. The tip indents the sample, which causes deflection on the cantilever. Such an indentation enables measuring the mechanical properties of the sample if the indentation is very small. Local indention results in a very high spatial resolution of the mechanical properties. With deeper indentation, the estimation of material properties becomes very difficult when the tip is a very sharp pyramidal type. To simplify the calculation of mechanical properties, conical, cylindrical, spherical, and wedge shapes of the tip have been introduced as shown in Figure 12. In this mode, the force can be kept constant to extract the mechanical properties of the sample. 2) In the noncontact mode, the tip hovers over the sample with a distance around 50−150 Å. A very low-
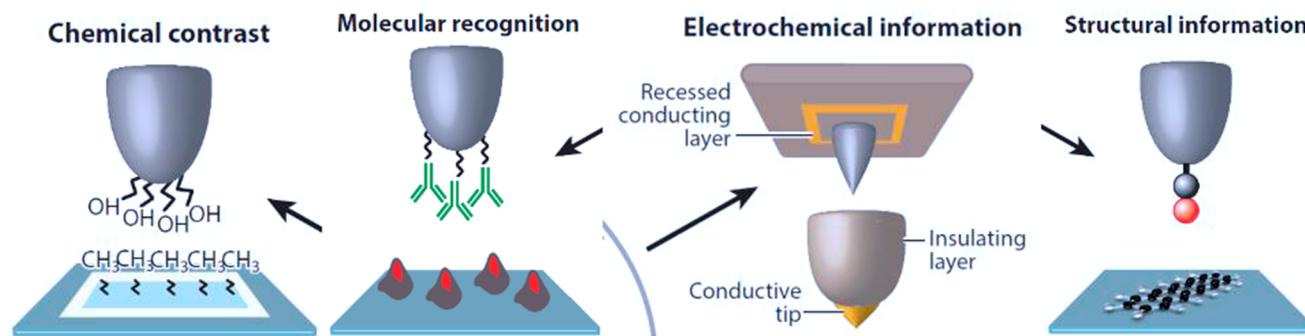
Figure 14. The tip of the AFM can be functionalized to perform other types of measurements in addition to the mechanical properties. Ligands and antibodies could be attached to the tip, and during the scan, they will bind to specific molecules for chemical contrast, molecule recognition, and structural information. If the tip has a conductive layer, it can detect electrochemical information from the surface of the sample. Adapted with permission from reference 78. Copyright 2018 Annual Review of Analytical Chemistry.

amplitude oscillation is delivered to the tip, and interaction between the tip and sample is measured by monitoring the change in amplitude of oscillation or shift in frequency. The cantilever detects long-range forces, such as van der Waals forces or electrostatic forces. Due to the nature of noncontact operation, the sample integrity is completely preserved. However, the noncontact mode produces images at lower resolution than contact mode. 3) In semicontact mode, which is also called tapping mode, the cantilever oscillates above the sample at a frequency close to the natural resonance frequency of the cantilever. The tip intermittently contacts the sample. Tapping mode effectively eliminates the influence of lateral force and reduces the force caused by absorption. It produces higher image resolution than noncontact mode as shown in Figure 13.

Environmental Conditions. AFM can be operated in an environment that is physiologically relevant to the sample. For example, the sample can be fully immersed in the buffer solution, and the temperature, pH, humidity, CO_2 concentration, and atmospheric pressure can be adjusted to obtain the native functional and properties of the sample as much as possible. For very soft material in buffer solution, the contamination with macromolecules from the sample and buffer solution can alter the interaction of the cantilever and sample. Therefore, routinely checking the contamination is necessary for biological applications.

Selection of Cantilever. Choosing the proper cantilever for the correct measurement of mechanical properties of the sample is crucial. The spring constant of the cantilever needs to be close to the elastic modulus of the sample. Otherwise, the force detection would not be sensitive enough for that particular material. If the cantilever is much stiffer than the sample, the deflection of the cantilever would be very small and not a good representation of the sample properties. If the cantilever is much softer than the sample, it will not indent the sample sufficiently to estimate the mechanical properties correctly. Procedures have been introduced to estimate the spring constant of the cantilever before an experiment. Variation in the depth of indentation will cause considerable differences between measurements.

Obtaining Viscoelasticity from Force−Distance Curves. Calculation of mechanical properties of soft matter from force−distance curves is not a trivial task, and still more models are proposed to account for the limitations of current models. Hertz, Derjaguin−Müller−Toporov, and Johnson−Kendall−Roberts models have been used often. Each model is

proposed for a specific cantilever and tip geometry. Some models do not consider the time dependency of the material. If the viscous modulus of the sample is the subject of investigation, then the models that account for time dependency should be considered. For time dependent materials, the loading rate is a critical parameter to quantify the viscous modulus. Some models take into account the effect of the adhesive and friction properties of the surfaces. There are also compounds to passivate the probe by nonadhesive molecules such as polyethylene glycol.

Multifrequency Imaging. Advanced noncontact mode includes frequency modulation, amplitude modulation, and multifrequency mode imaging, which offer higher frame rates to reduce the data acquisition time. Multifrequency imaging opens up exciting possibilities for studying biological systems. In this mode, the cantilever simultaneously excites and detects multiple harmonics of fundamental resonance frequency of the cantilever. The key idea is to relate the observables by AFM such as amplitude, phase, and frequency shifts of cantilever vibration to material properties such as topography, viscoelasticity, adhesion, flexibility, magnetism, or electrostaticity.

High-Speed Imaging AFM. In general, AFM imaging is a very slow process. The cantilever is the slowest component of the AFM and to achieve high speed imaging, the cantilever's response time needs to be reduced. Hence, smaller cantilevers are developed. Another factor that affects the speed of imaging is the mechanical vibration in the Z-direction. For this purpose, counterbalancing the impulse generated by quick z-displacements and actively damping the vibrations can be taken into account.

Multifunctional AFM through Functionalized Probes. In addition to examining the mechanical properties of the material by force spectroscopy, functionalizing the tip of the probe expands AFM applications to obtain chemical, electrochemical, and structural information and molecular recognition of the surface of the sample. Functionalizing the probe, as depicted in Figure 14, usually entails the covalent attachment of a specific molecule (ligands, antibodies) to the tip that can bind to specific molecules on the sample to map a specific interaction with the sample. This technique provides information about the localized receptors as well as binding forces, which can be measured in real time with topography. Some examples include quantifying cell adhesion, monitoring assembly and binding events of viruses, measuring kinetic and thermodynamics of ligand−receptor interactions, correlating

363

the structure and assembly of soluble proteins, and mapping a particular binding site.[64−66,68−77]

3.3. Nanoindentation

Nanoindentation is a point-probe-based technique where the probe indents the surface of the sample in the range of nanometers, while the applied force for such known indentation is measured precisely. Knowing the depth of indentation, the geometry of the probe, and the exerted force provide the information to extract mechanical properties of the surface of the sample. Nanoindentation is widely recognized as the preferred method for the thin film interfacial properties. Hence, there is a growing interest to study biological sample surfaces by nanoindentation. While there seems to be a similarity between AFM and the nanoindentation probe, the mechanism of sensing is very different. AFM measures atomic forces between the tip and the sample. In nanoindentation, external force pushes the tip of the indenter on the surface of the material, which creates a nanoscale impression referred to as a nanoindentation. The external force is measured and controlled, and the nanometer depth of indentation is measured along with the time that the force was applied and displacement occurred, as shown in Figure 15. The loading
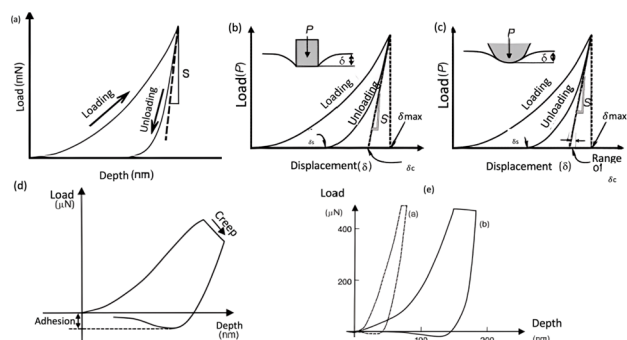
Figure 15. (a) Nanoindentation records stress versus displacement at the tip of the indenter and, based on the tip geometry, computes the mechanical properties of the sample. The difference between loading and unloading curves shows the hysteresis of the material, which is an indication of viscoelasticity. (b) and (c) depict different probe tip shapes which result in different load−distance curves. (d) and (e) If the material causes negative changes in the load-distance curve, the effect of adhesion should be subtracted from material mechanical properties. Adapted with permission from reference 79. Copyright 2005 Woodhead Publishing.

system that exerts pressure on the sample can be electrostatic, electromagnetic, or mechanical. Due to very small indentation, microscopy usually accompanies the indenting process to ensure the correct location of the point of interest. In the early days of development, nanoindentation was favored because it provided the material elasticity and its surface hardness. The load/unloading displacement curves provide critical information in the extraction of material properties. In addition to elasticity and surface hardness, other information about the deformation process can be obtained from them, such as fracture events, phase transformation, and the effects of temperature and surface chemistry on material properties. Some studies have shown that the material adhesion properties can be obtained using nanoindentation. The geometry of the tip is important in accurately calculating the material properties accurately. Various geometries are available, such as cones, pyramids, cubes, spheres, and paraboloids. The user needs to

pay close attention to the calibration process and the material that was used for the calibration. If the calibration was done with a material that shows very different properties than the sample under the test, the results will not be accurate. Most data analyzing techniques rely on unloading curve versus loading curve because, during loading, plastic properties of the material contribute to the force−displacement curve. But during unloading, only the elasticity of the material is the main component of the force−displacement curve. The more recent techniques add a small oscillating load component to the DC load, which causes the sample to act like a spring and a damper. Using this method, the viscoelasticity of the material in dynamic mode can be obtained by sweeping over a range of frequencies. Figure 16 depicts a schematic diagram of a nanoindentation setup.
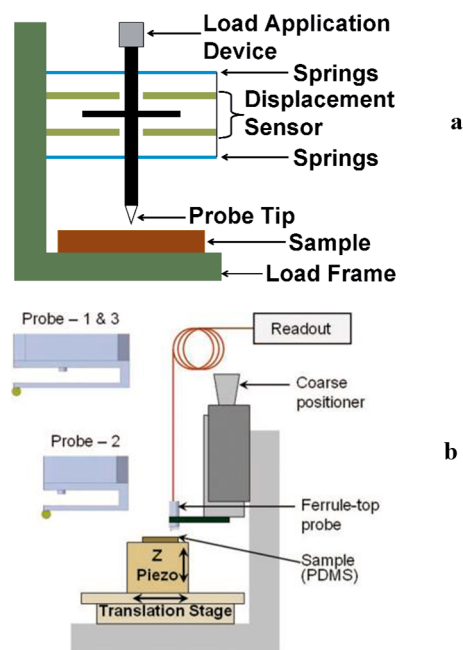
Figure 16. (a) A system diagram of the nanoindentation setup. The probe tip contacts the material and, based on displacement and the applied stress, force−distance curves are obtained. (b) The diagram of the recent nanoindentation device that is based on deflection of the ferrule and light interferometry. The tip of this device has a spherical shape and is more suitable for very soft materials such as hydrogels and cells. Adapted with permission from references 80 (Copyright 2003 National Institute of Standards and Technology) and 81 (Copyright 2012 Review of Scientific Instruments).

Anisotropic elasticity and plasticity of the bone and dental enamel have been studied by nanoindentation techniques. In some cases, the bone elasticity was measured in a liquid that requires the viscosity of the fluid environment to be considered during loading/unloading of indenter. For the soft biological materials, the viscous modulus and the adhesion properties of the surface of the sample will cause changes in deformation and loading/unloading−displacement curves that need to be taken into account when calculating the material properties.

Recently, instead of stiff probe and spring loading, a new technique that is based on a ferrule-top probe connected to a cantilever was developed that utilizes a fiber optic terminated with a spherical tip as the indenter. The deflection of the cantilever during loading/unloading is measured through light Fabry−Pérot interferometry. The force exerted on the sample

Induction of vibrations   **Dynamic response**   **Data processing and display**
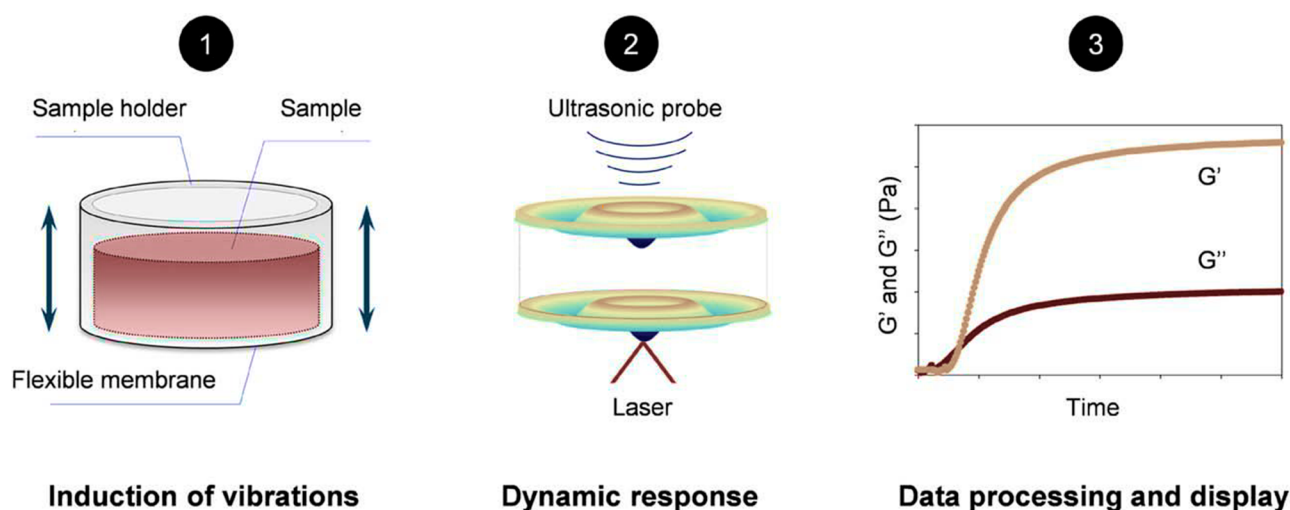
Figure 17. Representation of the series of processes needed to measure the sample viscoelasticity. (1) Diagram of the sample holder and the flexible membrane with known mechanical properties. The sample is loaded in the sample holder. The diameter and height of the holder are fixed dimensions. (2) After loading the sample into the machine, an ultrasonic probe vibrated the sample inside the holder. An optical system measures the displacement on the surface of the sample and calculates the viscoelasticity of the sample. (3) Elastic and viscous moduli are plotted over time, before, during, and after the gelation. The user can record how long the gelation takes time and how much the gel mechanics have changed. Adapted with permission from reference 83. Copyright 2017 Society for Biomaterials.

can be in the range of nano-Newtons. The resolution of the displacement is reported around 2 nm. Static and dynamic indentation can be applied to obtain the elastic and viscoelastic properties of the material.

3.4. Rheolution Instrument

In 3D cell culture and regenerative medicine where biomaterials are mixed with cells, sample preparation usually takes several days, and spending such an amount of time by specialized personnel makes the process costly. In some cases in which samples are made from primary cells, the sample is precious. For these reasons, destructive tests to obtain mechanical properties of the sample are not good options, and having a nondestructive test that can be sterile is very attractive. Rheolution Inc., a Canadian company, has commercialized a patented technology that measures the viscoelasticity of soft materials without mechanical contact. This technique uses a proprietary flexible membrane and a cylindrical sample holder with dimensions of 22.1 mm in inner diameter and 19 mm in height. It requires the sample to be pourable and have a volume of 0.5−0.7 mL. The gelation or cross-linking is expected to happen when the sample is poured in the holder. The flexible membrane vibrates, and its vibration is propagated to the sample. A laser-based imaging system detects the vibration at the surface of the sample as shown in Figure 17. The membrane and sample holder were characterized in terms of mechanical response to vibration. The only unknown factor is the sample in the holder. Models have been developed to obtain the elastic modulus and shear modulus from the combination of membrane vibration and laser detection of the sample. It has been reported that the viscoelasticity of the material can be measured in 3 configurations: 1) during a liquid-to-solid phase (gelation or polymerization); 2) during a steady solid state (hydrogels evolving over time); 3) during a solid-to-liquid phase (melting of degrading hydrogels).[82,83]

3.5. Optical Rheometry

Conventional ultrasound elastography and magnetic resonance elastography provide mechanobiology information at a spatial resolution of about 0.1−10 mm with a depth of penetration of a few centimeters. AFM probes materials with a resolution of nanometers. The spatial resolution gap between these methodologies and demand for noninvasive methods provide opportunity for optical techniques since they can provide spatial resolution of 5−15 μm and depth of penetration of about 2 mm. Several optical elastography methods have been proposed, such as Optical Coherence Elastography (OCE), Brillouin Microscopy, digital holography, laser speckle, and ultrasound-modulated optical tomography. For smaller-length scale samples in the range of 100 μm or less, multiple microrheology techniques have been proposed, such as passive microrheology, active microrheology, dynamic light scattering, diffusive wave spectroscopy, and optical tweezers.[84−87]

3.5.1. Optical Coherence Elastography (OCE). A combination of mechanical loading and optical coherence tomography (OCT) can provide information about the viscoelasticity of the sample. OCT is based on low-coherence interferometry and typically achieves a resolution of 5−15 μm in the axial direction, and the beam width of the laser determines the lateral resolution. 3D image acquisition of a volume with dimensions of 10 mm × 10 mm × 2 mm takes about less than 1 s. External loading is required in the OCE to generate the stress signal and deform the sample. Compression loading is a popular method, and it is typically applied in a stepwise and quasi-statical way (low speed) to avoid inducing detectable wave propagation. In compressional loading, the stress is assumed to be uniform across the sample, and measuring only the deformation provides a qualitative measurement of elasticity of the sample. The other form of loading is applying continuous oscillatory mechanical waves at the resonance frequency of the sample, which includes the geometry of the sample and its boundary conditions. The harmonics of the resonance frequency induce tissue motion which can be detected by an OCT. The geometry of the
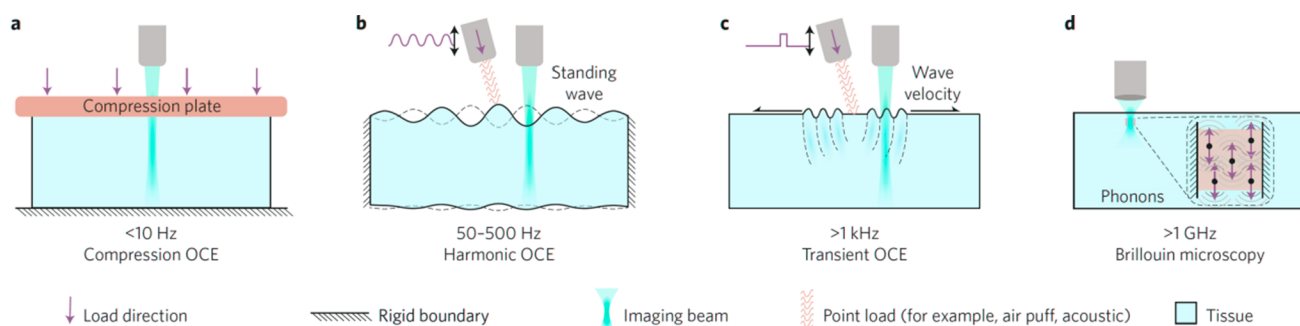
Figure 18. Various methods of excitation in the OCE and their comparison with the Brillouin method, which does not need external force. (a) A compression plate applies force uniformly on the sample and deforms it. Light coherent microscopy measures the deformation, and the instrument calculates viscoelasticity based on stress and measures strain. (b) An external force generator applies mechanical waves to generate standing waves in a defined boundary. OCE measures harmonics of standing waves to calculate the mechanical properties. (c) External mechanical waves are applied to the surface of the material, and shear wave velocity is measured, which is related to Young's modulus. (d) In Brillouin microscopy, there is no external force. Photons interact with phonons inside the sample and measure their vibrations. The Brillouin technique measures longitudinal properties, not the elastic or viscous modulus. Adapted with permission from reference 85. Copyright 2017 Nature Photonics.

sample and boundary conditions need to be known to extract material viscoelasticity from the tissue motion in higher harmonics. Transient mechanical loading using an indenter, acoustic radiation force, noncontact air jet pulse, or laser pulses can be applied to generate either surface acoustic waves (propagate only the surface of the material), shear waves (propagate deeper into tissue), or Lamb waves (propagate between two layers). Such a technique requires knowledge of material uniform density, local homogeneity, and its Poisson's ratio. These waves dissipate quickly in materials with a liquid content. Therefore, the loading should be scanned through the sample surface, which can be time-consuming. Figure 18 illustrates the basic differences between the OCE and Brillouin techniques.

Deformation detection in the OCE is done by two approaches: speckle tracking and phase-sensitive measurement. In speckle tracking, consecutive 2D or 3D images that are obtained at different loading conditions are cross-correlated to estimate the displacement. Cross-correlating 3D images gives an advantage to speckle tracking. Also, speckle tracking is less sensitive to tissue motion and artifacts but has lower resolution than typical OCT imaging. In phase-sensitive imaging, the Fourier-domain detection in the OCT offers interferometric optical phase imaging, which enables nanoscale particle tracking. The phase shift is proportional to the laser wavelength and inversely proportional to the refractive index of the sample. A phase difference of greater than 2π limits the measurable displacement, which requires the use of phase unwrapping algorithms. Phase-sensitive imaging is mostly done on axial displacement. To obtain viscoelasticity information, the lateral displacement needs to be incorporated with OCE.[84−86,88−93] Figure 19 depicts a system diagram of an OCE setup and compares it with other measurement techniques.

3.5.2. Brillouin Microscopy. Brillouin scattering was introduced in 1922 mainly for investigating condensed material properties. It offers an alternative assessment of elasticity through investigation of the longitudinal modulus at GHz frequencies. Its underlying physics principle is based on the interaction of light with spontaneous, thermally induced density fluctuations. These fluctuations are intrinsic to the material and described by a population of microscopic acoustic waves called phonons. So, unlike the case for an OCE, Brillouin microscopy does not need an external stimulus for
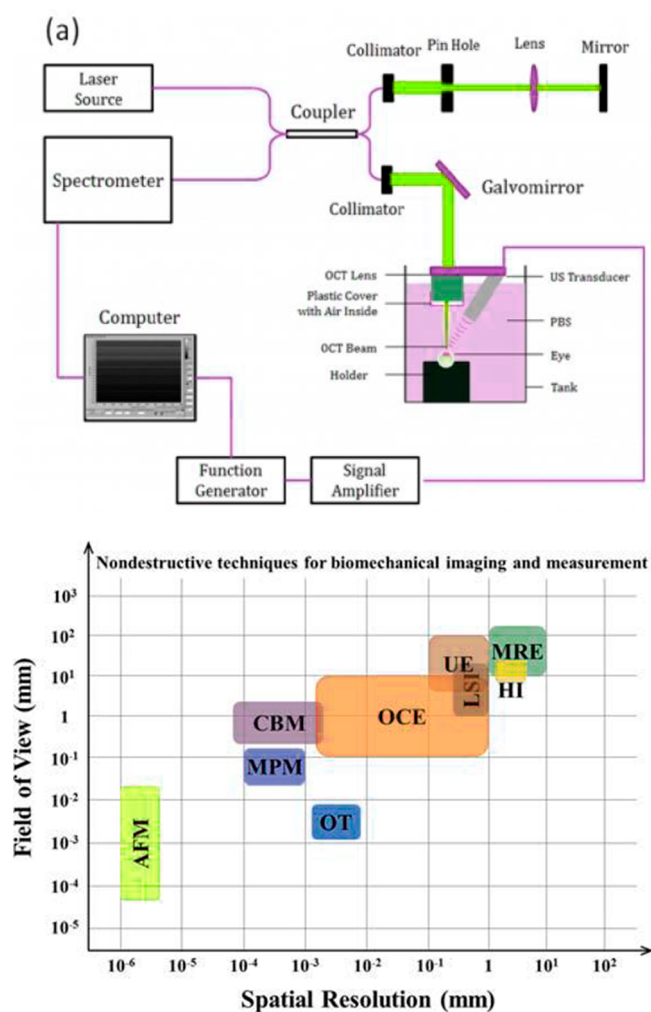
Figure 19. (top) Optical system block diagram of the OCE. (bottom) Comparison of the OCE with other viscoelasticity techniques over spatial resolution and field of view. AFM (atomic force microscopy), OT (optical tweezers), UE (ultrasound elastography), MRE (magnetic resonance elastography), MPM (multiphoton microscopy), CBM (confocal Brillouin microscopy), LSI (laser speckle imaging), HI (holographic imaging). Adapted with permission from reference 88. Copyright 2015 Wiley-VCH.

mechanical loading. Phonons collectively represent periodic excitation of the atomic and molecular densities in solids and liquids. The elastic scattering of light from a material has the same frequency as the light source. The elastic scattering of light is called Rayleigh scattering. However, a small portion of photons interact with phonons and exchange energy and momentum in their interactions. Phonons diffract light, and because they have traveling velocity, they change scattered light frequency by the Doppler effect. Doppler phenomena generate two additional frequency peaks in the scattering spectrum called Stokes and Anti-Stokes Brillouin peaks. For a material with known density and refractive index, these frequency shifts represent the material complex longitudinal modulus, for which the real part is the peak frequency and contains information about elasticity, and the imaginary part is the bandwidth of the Stokes frequency and has information about material viscosity, as depicted in Figure 20. It should be
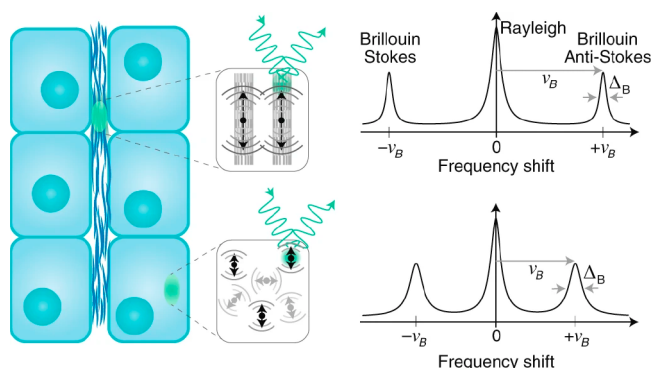
Figure 20. (left) Light scattering from a solid-like material (for example, collagen fibers) and liquid-like material (cytosol). (right) The Brillouin frequency shift is larger in solid-like materials compared with liquid-like materials, but the line width is smaller in rigid materials compared with liquid-like materials. Adapted with permission under a Creative Commons [CC-BY 4.0] from reference 97. Copyright 2019 Nature Methods.

noted that the longitudinal modulus is not the same as the shear modulus, and in order to obtain viscoelasticity of the material, the Poisson's ratio needs to be known. For soft materials in which Poisson's ratio is very close to 0.5, the longitudinal modulus is several orders of magnitude larger than the shear modulus, and quantifying an accurate value for viscoelasticity from the longitudinal modulus can be very challenging. The Brillouin spectrum is measured at GHz frequencies and requires an optical spectrum analyzer.

In cell mechanobiology, actin polymerization and branching of actin fibers can be studied by the Brillouin technique. Protein aggregation and liquid-phase-separated organelles lead to a differential Brillouin shift. Also, myosin contractility has been observed by a shift in Brillouin scattering. The change in Stokes peak bandwidth that is related to the viscous modulus of the material has not been attributed to any biological effect yet, and it remains an opportunity to be explored by future experiments.[94−102]

3.6. Microfluidic Rheometry

Microfluidic devices are essential for studying the behavior of complex fluids in micrometer-scale geometry. They have enabled the possibility of probing the bulk rheology of a fluid on a very small scale when the sample size is limited. They also provide the means to integrate the rheological devices with

other microfluidic lab-on-the-chip devices.[103] Bulk rheological properties can be measured in shear and extensional flow. Particle-based methods have been used to probe the local viscoelasticity response from nanoparticle motion in the fluid. They impose a defined boundary condition to study complex fluids such as crystal liquids.[104] In a typical microfluidic channel, at least one length's scale is smaller than 100 μm. Surface roughness, hydrophobic versus hydrophilic interactions at the wall interfaces, and electrical forces in ionic liquids could cause apparent slip and become the source of nonhomogeneity in the fluid that affects rheological measurements. For very low viscosity liquid, that elastic modulus may not be easily measured by other rheological measurement techniques, but in microscale geometries, the elasticity measurement is possible.[104]

Microfluidic devices possess several advantages over AFM, nanoindentation, noncontact tweezer technologies, and micropipette rheometry when it comes to single-cell analysis, especially for circulating cells in the bloodstream. They can be high throughput and cost-effective and are not technically difficult to implement. Similar to flow cytometry, they can be used in clinical settings as well. All three forms of microfluidic devices have been shown to be effective in measuring single cell deformability by a change in osmotic pressure. However, only capillary and contraction point flow devices have the ability to detect actin disassembly.[105] A combination of microfluidic devices with controlled acoustic fields has been explored in microfluidic acoustophoresis techniques, and it has been shown that it can increase the resolution and sensitivity of cell separation in circulating tumor cell (CTC) devices.[106,107]

As depicted in Figure 21, in the capillary configuration, the cells flowing in the microfluidic channel change their shape
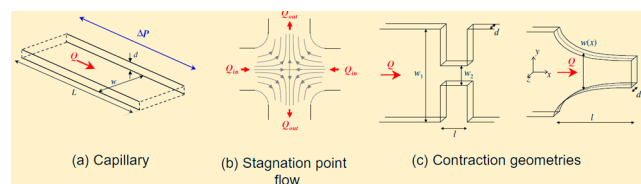
Figure 21. Three configurations for microfluidic devices have been introduced to measure rheologically complex fluids. (a) The capillary devices are used for measuring shear viscosities. The viscosity is a function of flow rate Q and pressure drop ΔP throughout the length of the channel L. w and d represent the width and depth of the channel, respectively. Two main approaches of controlled pressure drop and controlled flow are identified for capillary viscometry. Viscosities in the range of 0.001−10 Pa·s have been measured over a range of shear rate of 0.1−0.001/s. In some cases, a sample volume in the range of nanoliters was successfully measured. (b) The stagnation point flow is used for extensional deformation. Near the stagnation point, the flow is in a vorticity-free state, which can result in orientation of the microstructural components of the fluid. Video or fluorescent microscopy is used for observing the flow birefringence at the stagnation point to obtain the rheological information. (c) Contraction devices measure the sudden pressure drop in an imposed flow. Adapted with permission from reference 104. Copyright 2009 Elsevier.

from a circular particle to an oval-shaped particle. The deformability of the cell is defined by its deviation from a perfect circle. The deformability of the capillary device is not as large as that of the stagnation device. In the stagnation point flow, the cells are under stress from two flows in opposite

directions, which causes elongation in the axial direction and shrinkage in the lateral direction. The cell deformability is defined by the aspect ratio of the changes in the axial and lateral directions. In contraction geometry, cells are under stress in the narrowed channel, and the time of passage from the channel defines the deformability of the cell.[105]

3.7. Micropipette Aspiration Rheometry

Since the 1970s, micropipette aspiration has been used to conduct studies on biological tissue mechanics. This technique includes a micropipette that is positioned very close to the material of interest (almost in contact with it) and is connected to a pump or water reservoir to create negative pressure plus the imaging setup (microscopy). A pump applies the negative pressure to the tip of micropipette and pulls the material into the pipet as depicted in Figure 22. Biomechanical models have been developed to extract viscoelasticity of the material by measuring the negative pressure and the displacement of the material into the pipet.
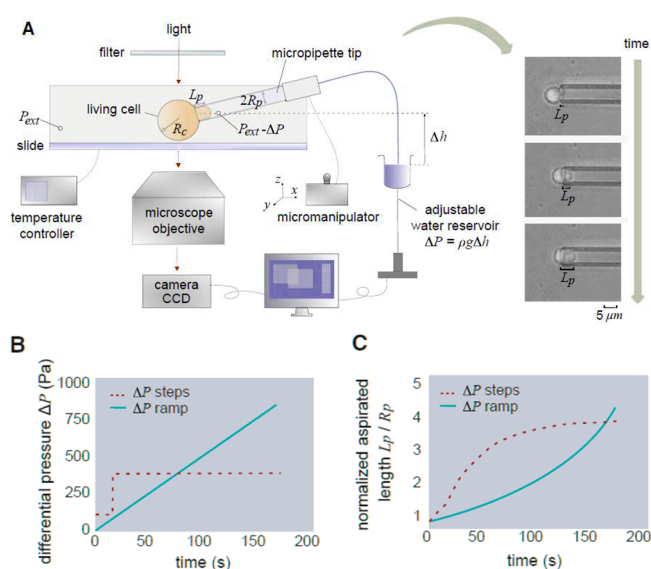
Figure 22. (A) A simple diagram of the micropipette aspiration technique. By applying negative pressure to the tip, the particle will gradually move into the pipet. The experiment is done either by constant pressure or by constant ramp pressure. (B) The pressure changes either in step function or by a ramp function over time. (C) The length of the material drawn into the pipet changes over time, and the curve of change of the length depends on the change in pressure. Adapted with permission from reference 108. Copyright 2019 Biophysical Society.

Usually, two types of experiments are defined by micropipette aspiration: 1) constant pressure similar to the creep test and 2) ramp pressure similar to constant shear rate. The aspirated length is measured over time. Depending on the aspirated length and time of aspiration, different models for viscoelastic and poro-viscoelastic materials are proposed where the porosity of the material makes a significant difference in measurements. Versatility and ease of use of pipet have allowed additional measurements to be done by micropipette, as shown in Figure 23. Examples are 1) using microindentation to probe the local mechanical properties of the cell, 2) including florescent and confocal microscopy to observe biomolecules during mechano-sensing activities, 3) using functionalized coated beads to assess push/pull forces of a cell, 4) measuring

the required force to detach a cell from substrate, 5) studying cell−cell attachment forces during morphogenesis using two micropipettes, and 6) measuring surface tension forces in a growing cell aggregate.[108−113] Recent advancements have allowed the use of optical interferometry with micropipettes to obtain subnanometer spatial resolution[114]

3.8. Interfacial Shear Rheometry

Interfacial rheometry studies the 2D deformation or response of an interface to shear stress. The interface could be liquid−liquid, liquid−gas, liquid−solid,[115] and solid−solid.[116] In biology, interfacial rheometry has applications in biofilm, monolayer[117] or bilayer lipid, membrane, and alveoli[118] rheology. For example, oxidative damage to lung epithelial cells and air-pollutant-induced lung surfactant damage have been studies by interfacial shear rheometry.[119] Another example is the rheological properties of the tear film. A uniform tear film that sustains the hydration of the cornea is critical for ocular health. The effect of lens care solutions on tear lipid rheology has been studied since some surfactants can destabilize the tear film and cause the emulsification of the lipid layer of the tear film.[120] Interfacial rheology has been used to study the protein adsorption at multilayer and single-layer surfaces at the aqueous-buffer−air interface.[121] Viscoelasticity of a thin polymer layer on a solid can be studied by interfacial rheology as well as how a liquid drop sits or moves on a substrate material which can be useful for 3D bioprinting.[122]

3.9. Biomolecular Rheometry

Molecular tension sensors are an emerging technology that overcomes certain limitations of AFM and tweezers rheometry techniques to investigate the intracellular mechanism of force transduction (AFM and tweezers are mainly applicable to the cell surface). They enable detection of a few pico-Newtons force experienced by an individual protein in a living cell, organoids, and organisms at single-molecule resolution. This technique utilizes Förster resonance energy transfer (FRET) to monitor changes in the applied force and displacement. So far, two types of sensor molecules have emerged: genetically encoded tension sensors, which are protein biosensors with sensitivity to forces below 10 pN, and synthetic tension sensors, which have been synthesized using poly(ethylene glycol) (PEG), nucleic acids, and proteins. Synthetic sensors can detect forces between 4 and 100 pN and are used to study cell surface receptors and cell−cell interactions. Generally, three categories of polymer behavior have been considered for molecule tension sensors as depicted in Figure 24. The first category is a well-solvated polymer called entropic-spring behavior. The tension sensor consists of a flagelliform linker sequence polymer flanked by fluorophores. By applying tension to this sensor, the linker is extended, and the fluorophore is moved away from the quencher, which causes a measurable increase in fluorescence. The second category is also a well-solvated polymer, but its behavior is a switchlike extension behavior. Examples of these polymers are DNA duplexes, DNA hairpins, and proteins. They are folded constructs in 3D, and their unfolding shows a sudden change in displacement in response to a narrow range of forces. The third category is unsolved polymers. They require a large force to extend beyond the force employed in biology; therefore, this type is not practical for studying biological systems. The microscopy readout can be based on the fluorescence intensity, ratiometrics, fluorophore lifetime, fluorescence polarization, super-resolution microscopy, and multivalent tension sensors.
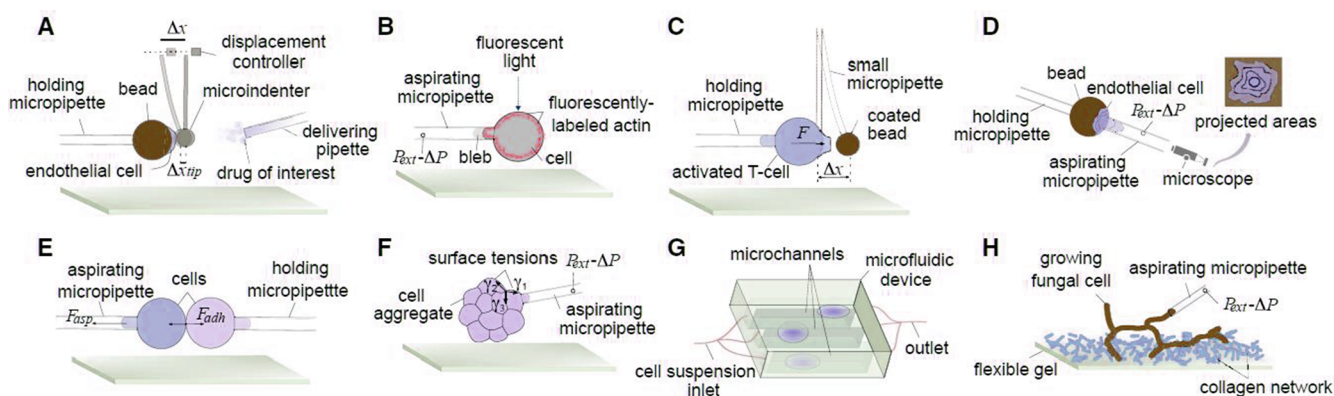
Figure 23. The micropipette aspiration technique can be combined with other technologies such as (A) microindenter, (B) fluorescent labeling, (C, D, E) secondary pipet, (F) spheroid manipulation, (G) microfluidic devices, and (H) branches of biopolymers or growing fungal cell. Adapted with permission from reference 108. Copyright 2019 Biophysical Society.
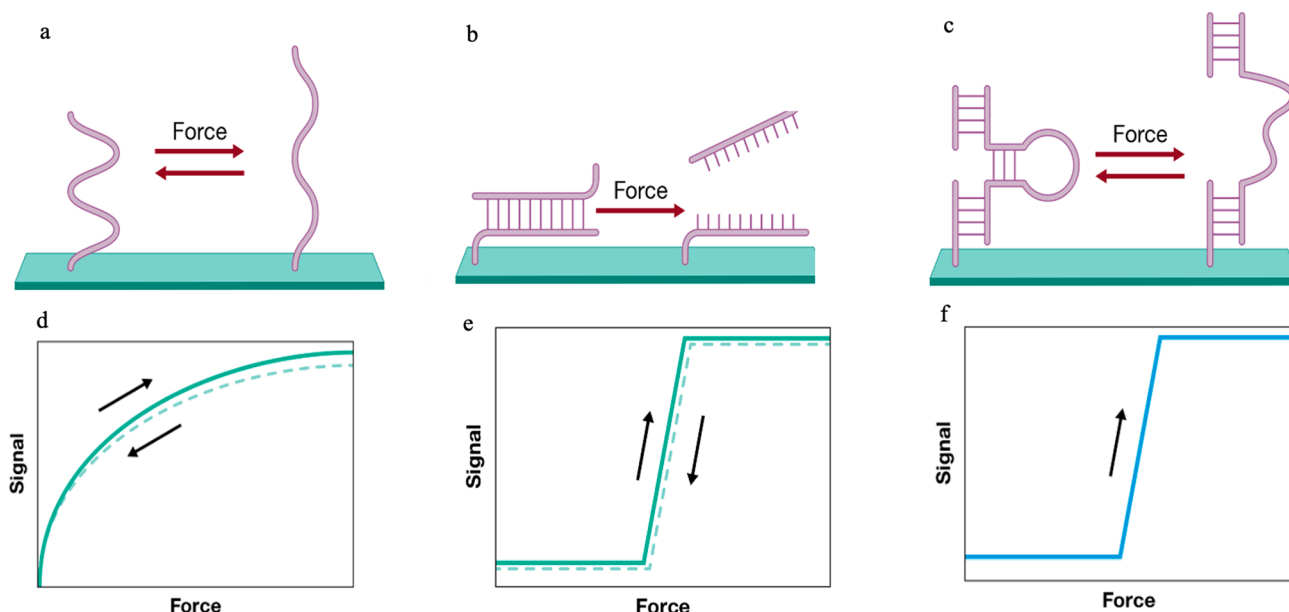
Figure 24. (a) PEG and genetically encoded tension sensor extension. (b) Tension gauge tether rupture. (c) DNA hairpin extension. (d) Change in force of genetically encoded tension sensors translates into an analog change in fluorescence. (e) Rupturing the tension gauge causes an abrupt (digital) change in fluorescence that is reversible. (f) Change in DNA hairpin force translates into a digital and irreversible change in fluorescence. Adapted with permission under a Creative Commons [CC-BY 4.0] from reference 123. Copyright 2021 ACS.

The nonmicroscopy readout methods include flow, catalytic amplification, and TGFβ Aptamer.[28,123−129]

3.10. Microrheology

When the sample size is extremely small, most forms of rheology techniques are not applicable. On the other hand, providing information at the microscopic level for heterogeneous materials is valuable to understand the interplay of various molecules within the bulk of the material. For these reasons, several noninvasive microrheology techniques have been developed that utilize micron-sized particles as probes to locally deform the sample. There are two broad classes of manipulation of these particles: a) one uses external forces and actively moves the particles, and b) the other one measures the passive motions of the embedded particles which are due to local thermal fluctuations or Brownian movements. These two classes are called active and passive microrheology, respectively. External forces applied in active microrheology are in the form of radiation forces for small particle manipulation such as magnetic, optical, and ultrasound tweezers.[130−132]

3.10.1. Magnetic Tweezers. Magnetically manipulating a paramagnetic or ferromagnetic micrometer-sized probe embedded in a material is the oldest implementation of microrheology. The magnetic probe is manipulated by external magnetic sources that generate gradient forces due to their distance to the particle. Often, two or four external magnetic sources are used to create a relatively uniform magnetic field in the region of interest. The movement of the particle is observed by video microscopy to assess the displacement of the probe. If only one magnetic particle is embedded in the material and one external magnet is used to move the probe, then the experiment is a qualitative measurement of the rheological properties. To obtain quantitative measurement of the viscoelasticity of the material, either Hall sensors need to be embedded into the material to measure the magnetic force at the location of the particle, or at least two external magnets are needed to have a uniform magnetic field and consequently

a constant force on the particle to compute the viscoelasticity parameters. The force scale in magnetic tweezers is in the range of pico- to nano-Newtons, and the particle displacement is in the range of 20 nm to a few microns. Magnetic tweezers have been used to investigate the viscoelastic properties of actin filaments,[133] cytoplasm,[134] fibroblasts,[135] macrophages,[135] endothelial cells,[136,136] dictyostelium cells,[137] viscoelasticity change in collagen matrices during fibroblast-collagen contraction,[138] and 2D protein network at liquid interfaces.[139]

3.10.2. Optical Tweezers.

Optical tweezers (trapping) were developed in the 1970s, and they are used to trap a micrometer-sized particle for micromanipulations such as applying forces at the level of pico-Newtons and measuring the displacement in the range of nanometers. The size of the bead must be either much smaller than or near the wavelength of the light. When the bead is much smaller than the wavelength of the light, it experiences almost a uniform electric field that induces polarization on the bead as a simple dipole. The dipole will respond to the movement of the electric field and follows it, as shown in Figure 25. That is the principle of optical trapping in the Rayleigh regime for particles much smaller than the wavelength.
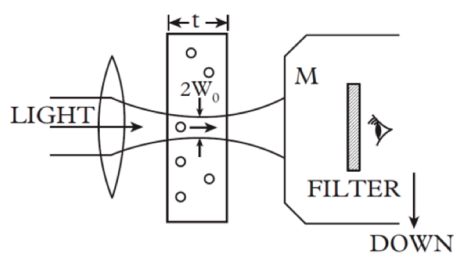
Figure 25. Schematic of the optical path and the converging beam. The focal point is aligned with the center of the material thickness. Adapted with permission under a Creative Commons [CC-BY] from reference 140. Copyright 1970 Physical Review Letters.

When the size of the bead is close to the wavelength of the light, the ray optics regime explains the trapping process. The reflections and refractions of the light impinging on the bead cause a change in momentum. The summation of all of the rays gives a gradient force to the particle that pulls it toward the center of the trap. That is how the particle can follow highly focused light.

The optical trapping instrument is relatively complex, as shown in Figure 26. Single-particle trapping provides viscoelasticity information on a local region where the bead is embedded. If necessary, molecules can be tagged, and using fluorescent microscopy visualizes the molecule of interest's movements. Two-particle trapping can provide viscoelasticity information at the macro scale. Since most materials of interest are not a continuum but have networks of macromolecules, the mesh and pore size of the network is important for bead selection. The bead should be about 3 sizes larger than the mesh size, and the surface of the bead should be coated with neutral polymers to avoid adhesion of the bead to the material. Figure 26 demonstrates a schematic of the instrument for microrheology experiments. The back focal plane force detection is achieved via a condenser and position sensing detector (PSD). Precision movement of the trap relative to the sample is achieved via a piezoelectric stage and/or mirror (GM-1). The mercury arc lamp, fluorescence filter cubes, 1064

nm dichroic, and CMOS camera are needed for fluorescence imaging. The polarization beam splitters (PBS), the second mirror (GM-2), and second PSD are needed for two traps. The remaining components are standard for optical tweezers.

To measure the linear viscoelasticity of the material, the trapped bead is sinusoidally oscillated by a wide range of frequencies to generate dynamic stress/strain fields, and by measuring the stress and strain, material properties can be extracted. To measure the nonlinear viscoelasticity of the material, large-scale displacement can be made by either a constant shear stress rate or constant strain rate. One method to perform a creep/relaxation test is to displace the bead in large-scale and with a constant strain rate and then turn off the laser and record the recoil of the bead. Measuring the time of recoil provides relaxation over time curves, and viscoelasticity parameters can be obtained from the curves. The bead can be functionalized to bind to a macromolecule to investigate the interactions among its constituents. Optical tweezers can be incorporated with microfluidic perfusion devices to study changes in the mechanical properties of the material while undergoing a chemical reaction. Optical tweezers have played a crucial role in investigating properties of biopolymers such as DNA, actin, microtubules, intermediate filaments, and worm-like micelles.[87,130,131]

3.10.3. Acoustic Tweezers.

Acoustic tweezers offer another contactless technique to apply a mechanical pressure field to a small particle for the purpose of trapping and manipulating it. Acoustic tweezers can be used for length scales from 0.1 μm to 10 mm with a power level as small as 10 mW to avoid damage to the cells. Originally, they were used for particle levitation and sorting. If the particle (bead) is functionalized, then it can be used for interrogating cell mechanics. Some studies have shown the use of a single ultrasound transducer with highly focused beam to study cell mechanics, as depicted in Figure 27. The pressure field can be generated by a single transducer, an array of transducers, and interdigit transducers. The underlying physics behind acoustic tweezers is very similar to that of optical tweezers. The summation of refractive and reflective fields pulls the particle to the center of the pressure field. Recent advancements with metamaterial reflective surfaces have enables researchers to generate acoustic levitation of multi-particles with arbitrary distances, which can be used for high throughput processes.[141−149]

3.10.4. Passive Microrheology.

Unlike the tweezers rheometry that use an external force to manipulate a particle inside the material of interest, passive microrheology does not require an external mechanical force but relies on Brownian movements of the embedded particles due to thermal fluctuations. The Generalized Stokes−Einstein relation explains the basic principle of passive rheometry. The Brownian movements of the particle probes depend on the temperature, the size of the particle, and the stiffness of the material. It is important to note that the particle movement in passive microrheology is 3D, and the mean-squared displacement is usually measured as a value that reflects the strain that accumulates due to thermal stress. A micrometer-sized particle moves about 0.1−10 nm in a very soft material and allows elastic modulus measurement of up to 500 Pa. Passive Microrheology has a smaller range than active rheology, but it has the advantage of measuring the linear viscoelasticity regime because no external forces are used. To measure the movement of the particles, techniques such as dynamic light

PBS = polarization beam splitter
PSD = position sensing detector
GM = gold mirror
L = lens
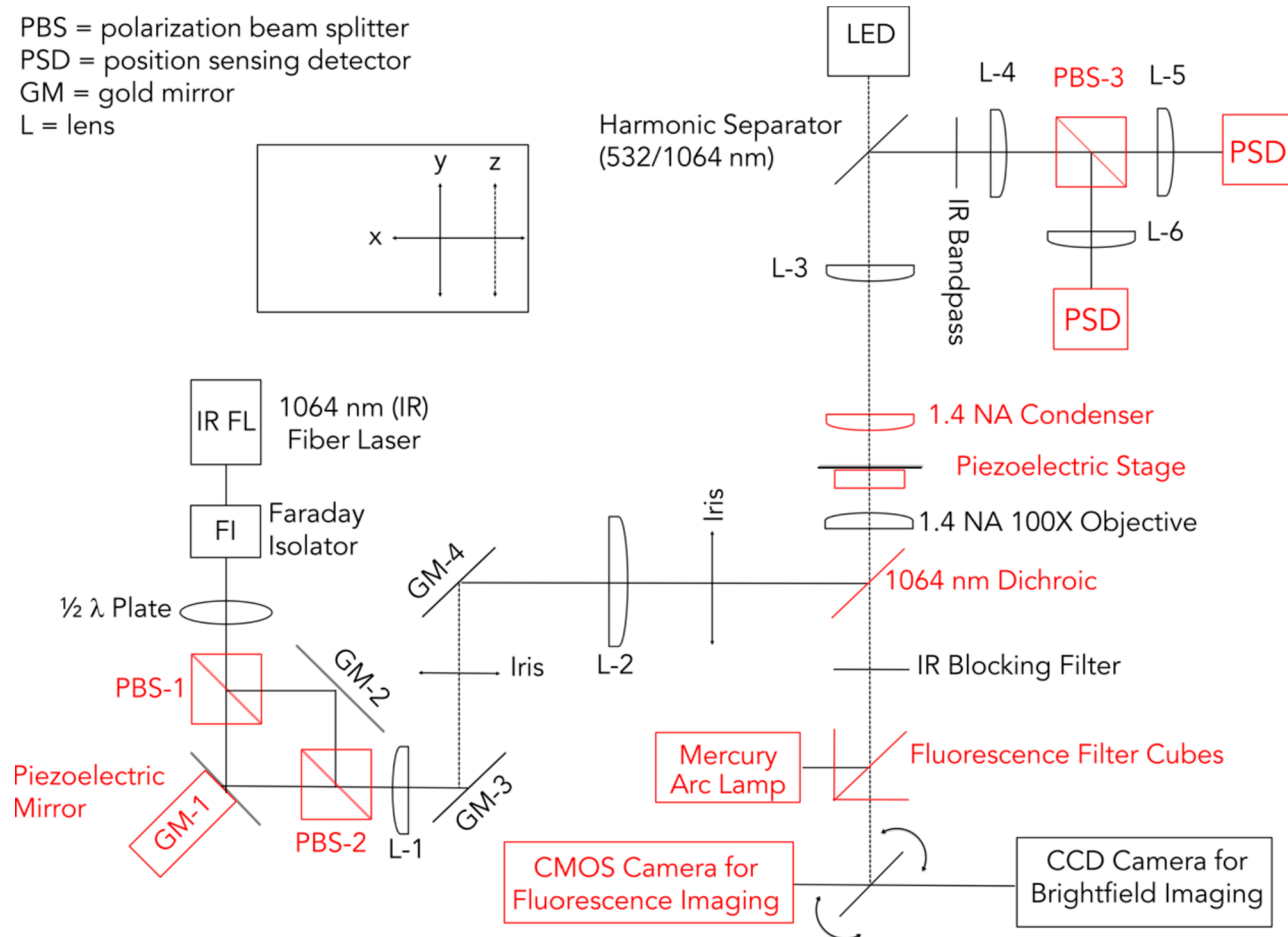
Figure 26. Basic schematic diagram for optical trapping. Adapted with permission from reference 87. Copyright 2018 ACS Macro Letters.
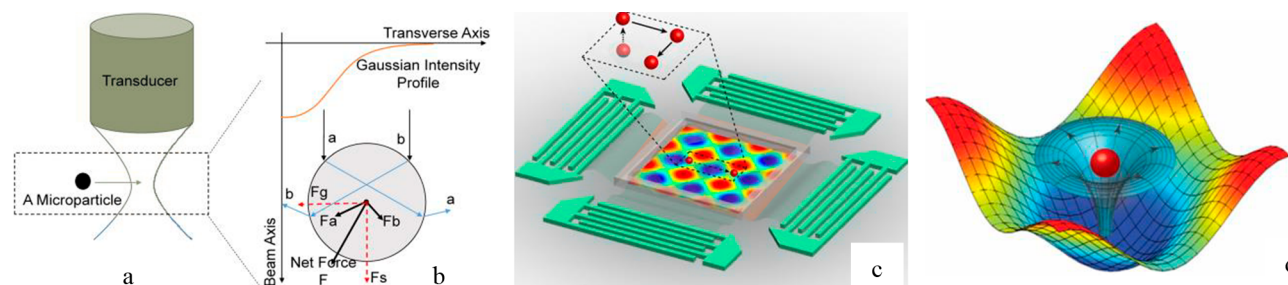
Figure 27. (a) Illustration of the focused acoustic beam in the vicinity of the particle. (b) Configuration of trapping forces applied to the particle. (c) A pair of interdigit transducers to generate a planar standing-wave field for 3D manipulation of a particle. (d) Numerical simulation of an acoustic beam near the particle in 3D. Adapted with permission under a Creative Commons [CC-BY 4.0] from references 147 (Copyright 2015 Elsevier) and 144 (Copyright 2018 Nature Publishing Group).

scattering, diffusing wave spectroscopy, interferometric tracking, and video microscopy have been used. In the dynamic light scattering technique, a coherent laser beam illuminates the sample and scatters. A detector with an angle to the axis of incident laser beam collects the scattered light. The scattered light is generated from many single scatterers that cause a random diffraction pattern called a speckle. The movement of particles changes the intensity of light in the speckle pattern over time, and using the Generalized Stokes–Einstein relation, the mechanical properties of the material are computed. The dynamic light scattering technique is used when the media is transparent or mildly opaque.

If the sample is translucent or highly turbid, diffusive wave spectroscopy is used. Diffusive wave spectroscopy solves the problem of multiple scattering inside the sample; therefore, the scattering angle is unknown. Diffusive waves are solved in two distinct geometries: transmission and backscattering. The optical setups for these two geometries are different. In the transmission geometry, the light decays faster than backscattering, which can translate into the transmission geometry reporting the microscale rheology of the sample better than the backscattering geometry. Passive microrheology is mostly used to measure polymer, surfactant, and protein solution rheological properties. Diffusive wave spectroscopy can be used to measure the longest relaxation time of entangled

polymer solutions. That requires measuring weak rheological properties and short time scales of the relaxation time, which are important in elastic instabilities in microscale flows such as microfluidic processes. Obtaining short time scale relaxation is attributed to high frequency rheometry that reveals information about the smallest filaments within the sample. This technique is used to measure viscoelasticity of F-actin filaments, rod-like viruses, and other supramolecular assemblies and macromolecular proteins that are semiflexible polymers.[130,131]

3.11. Ultrasound Elastography Techniques for In Vivo Models

Recently, ultrasound elastography has been widely used to measure tissue stiffness. Tissue characterization is useful in early stage disease detection when morphological changes may not be so apparent. It could also improve the accuracy of diagnosis by evaluating the size of the lesions and the level of progression. Also, it could provide some assessment of the response to certain treatments such as radiofrequency ablation and chemotherapy. Mapping the stiffness can provide valuable information for physicians with relevant diagnostic values. There is an intuitive, practical, and simple relationship between palpation and elastography. Wherever the palpation has been shown to be relevant, elastography can be considered as a diagnostic tool. The advantages of elastography versus palpation are that elastography does not depend on the experience of the clinicians since it is a quantifiable technique, and it can be applied in deeper tissue where palpation is not feasible.[150−162] Clinical ultrasound elastography applications include assessing liver fibrosis in chronic liver disease,[152,157] assessing malignancy of masses in the liver, breasts, kidneys, thyroid, prostate, and lymph nodes,[157] evaluation of peripheral nerves,[155] assessing tendon injury,[153] identifying disorders presenting with cardiac or muscle pathology,[150,151] and assessing plantar fascia[150] and ligaments.[150] In commercial ultrasound imaging machines, the elastic modulus is obtained either by Acoustic Radiation Force Impulse (ARFI) or the Shear Wave Imaging technique. In ARFI, Young's modulus is obtained by

$$E = \sigma/\varepsilon$$

and in Shear Wave Imaging, Young's modulus is obtained by measuring the propagation speed of shear wave:

$$E = 2(1 + \upsilon)G = 3G = 3\rho C^2$$

where υ is the Poisson ratio of the tissue, G is the shear modulus, ρ is the density of the tissue, and C is the shear wave propagation speed in the tissue. It is assumed that the Poisson ratio for incompressible material is almost 0.5 and constant. Also, it is assumed that the density of the tissue is known and constant. Other terms used for these two techniques are strain imaging or quasi-static imaging for ARFI and the dynamic method for shear wave imaging.

Elastography can be categorized by the excitation method and measured physical quantity such as follows: 1) Strain elastography: In this method, the strain values within the region of interest are displayed, and the excitation is a quasi-static method. It is a qualitative method. 2) Acoustic Radiation Force Impulse (ARFI): Focused pulses are applied to the specified region, and the displacement due to the excitation is measured. It is similar to strain imaging, and it is also a qualitative method. 3) Shear Wave Speed Measurements and

Imaging: Acoustic radiation forces are applied as pulses with a short duration of time, and the generated shear waves within the region of interest is measured. The information is presented as either shear wave speed or Young's modulus, or an image is generated by that information. 4) Transient elastography: A controlled excitation pulse is applied to generate a shear wave, the speed of propagation of the shear wave is measured, and Young's modulus is calculated. Figure 28 depicts these techniques. It is mostly used for liver tissue. It
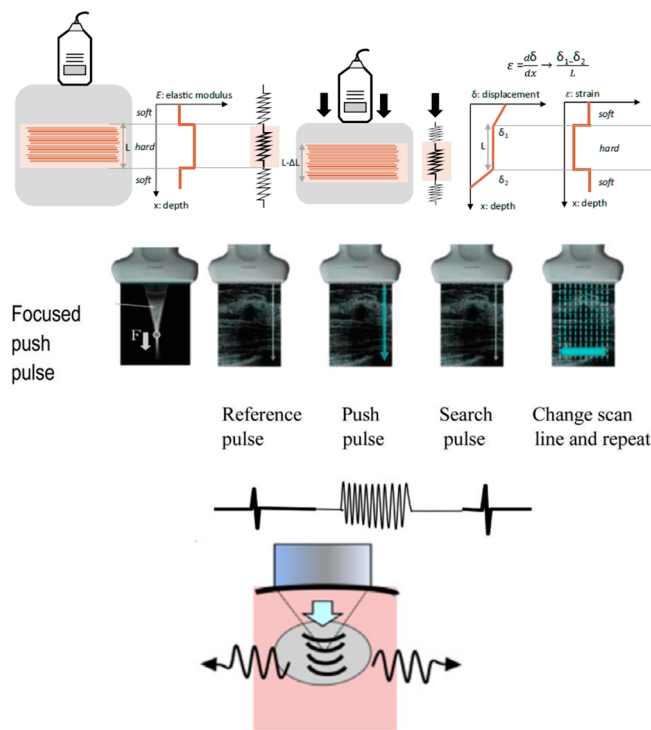
Figure 28. (top) Strain elastography method. (middle) ARFI. (bottom) Shear Wave Measurements. Adapted with permission under a Creative Commons [CC-BY 4.0] from references 153,162. Copyright 2018 Springer Nature. Copyright 2015 Elsevier.

is not used for imaging. In breast cancer diagnosis, the elasticity of the mass is scored in a five-point scale to classify the mass from benign to malignant as follows: score 1 (benign), score 2 (probably benign), score 3 (benign or malignant is equivocal), score 4 (malignancy suspected), and score 5 (malignancy strongly suggested). In the case of cysts, because the level of the internal echo signals from a cyst is low, it can be used for cyst diagnosis, like a lateral shadow or posterior enhancement on typical ultrasound imaging.[152−163]

3.11.1. Limitations and Artifacts in Ultrasound Elastography. Biological tissues are known to be nonlinear, heterogeneous, and viscoelastic. Due to these mechanical properties, the propagation of acoustic waves in these materials is very different than what has been modeled by linear, homogeneous, and elastic materials. Just including the effect of viscosity implies that the stiffness and shear wave speed depend on the excitation frequency and is known as dispersion. Dispersion is one reason why there are differences between various commercial systems in shear wave imaging. Nonlinearity of the tissue indicates that the response to stress depends on the initial strain of the material. Therefore, the values of strain depend on tissue compression, which happened in both strain imaging and shear wave imaging. Some studies

Table 1. Comparison of the Various Rheometry Methods

Method	Applied Force Range	Displacement Range	Site of Measurement	Sample Size	Examples
Rotational Plate	mN	mm	Bulk	10–20 mm	Gel, hydrogel
AFM	pN	0.01 nm	Surface	Atomic scale	Biopsy, gel, hydrogel, organoid, cell, cell organelle, protein, antibody
Nano Indentation	nN	2 nm	Surface	μm	Cell, gel, hydrogel
Rheolution Instrument	mN	μm	Bulk	20 mm	Gel, hydrogel
OCE	nN–mN	~ 10 μm	Map	μm–mm	Cell, ECM, organoid, biopsy
Brillouin	N/A	N/A	Map	Molecular scale	Actin, myosin, cell, organoid
Microfluidic	nN–μN	μm	Bulk	μm	Circulating cells
Micropipette Aspiration	nN–μN	μm	Bulk	μm	Cells, macromolecules, organoid
Interfacial Shear	nN–μN	μm	Surface interface	μm	Cell membrane, tear drop
Biomolecular	pN–nN	pm	Molecule	nm	DNA
Magnetic Tweezer	pN–nN	nm–μm	Surface	μm	Cells, ECM, organoid
Optical Tweezer	pN	nm	Molecule	nm–μm	Cell, DNA, actin
Acoustic Tweezer	μN–mN	μm–mm	Surface	μm	Cells, ECM, organoid
Passive Microrheology	pN–nN	nm	Bulk	μm	Actin filament, macromolecules
Ultrasound Elastography	μN–mN	μm	Bulk	mm	Tissues, biopsy

have shown that increasing transducer compression during breast and prostate cancer measurements resulted in increasing shear wave speeds. That is why applying minimal compression is desirable to improve the reproducibility of the shear wave technique. Nonhomogeneity of the tissue can cause artifacts and leads to incorrect shear wave estimation. Especially at the structural interfaces, the reflection of the shear wave could result in a soft center artifact in a very stiff lesion. It is recommended to exclude the structural boundaries that can be recognized by B-mode imaging when performing shear wave imaging.[164–166] The use of ultrasound technology in assessing mechanical properties of biologics and biological tissues have been limited to acoustic tweezers[141,142,144,147–149,169] and acoustofluidic devices in cytometry.[106,107] Ultrasound elastography requires a lot of elements in the probe to apply force and measure displacement of the region of interest. This has limited the use of ultrasound in in vitro and ex vivo models. However, due to the nature of noncontact assessing of tissue mechanics by ultrasound elastography, there is increasing interest in developing miniaturized ultrasonic probes to measure viscoelasticity of complex whole tissues and of 3D constructs from tissue engineering applications and from cell therapy modalities, such as soft biomaterials designed to deliver cells into host tissue for biomimicry and regenerative medicine.[157–168]

3.11.2. Comparison Table of the Discussed Techniques. To guide researchers on their choice of tools for measuring rheological parameters across different biomaterials, Table 1 provides a succinct comparison of the different the aforementioned viscoelastography techniques mentioned above. Because Table 1 summarizes the most basic features of these techniques, researchers are cautioned to carefully consider special attention should be the geometry of the sample and the environment of its natural state so as to define boundary conditions that approximate the real case for optimal biomimicry. In particular, cells that are dynamic and adapt their actin polymerization to different environments should be measured in a manner that represents the endogenous state or host tissue. For example, circulating cells in bloodstream are best measured in a microfluidic channel, and adherent cells are

preferred to be measured by AFM or OCE. Also of note, some techniques measure the viscoelasticity of the sample in a bulk (volume) format, meaning that all the components inside the sample contribute to its viscoelasticity and the measured values represent a homogeneous material with such viscoelasticity values. An example of such a technique is rotational plate rheometer. If the material is a homogeneous gel or hydrogel, bulk measurement is acceptable. But, if the material is heterogeneous such that mapping the variances in viscoelasticity across the sample provides more insight, then techniques that can provide spatial information on the sample's viscoelasticity should be considered.

4. APPLICATIONS

4.1. Regenerative Medicine

NIH refers to regenerative medicine as the process of replacing or regenerating human cells, tissues, or organs to restore or establish normal function. The promise of regenerative medicine is to regenerate damaged tissues and organs in the body by either replacing the damaged tissue or stimulating the body's own repair mechanisms to heal tissues or organs. If the body is unable to heal itself, laboratory-grown tissues and organs may be generated and safely implanted into the damaged tissue. Approximately one in three Americans could potentially benefit from regenerative medicine. Examples of regenerative medicine include cell therapies (the injection of stem cells or progenitor cells); immunomodulation therapy (regeneration by biologically active molecules administered alone or as secretions by infused cells); and tissue engineering that consists of transplantation of laboratory grown organs and tissues such as bone, cartilage, blood vessels, bladder, and skin. Often, the tissues involved require certain mechanical and structural properties for their proper functioning. Some cell therapy techniques require biomaterials to support the injected cells. The mechanical properties of the material are critical for cell survival, retention, and functionality. Table 2 lists notable tissue-engineered products that are either approved through clinical trials or are advancing through the approval process. These products could potentially benefit from the inclusion of

Table 2. Examples of Tissue Engineered Products in the Market or Clinical Trial

	Product	Tissue Type	Composition	Indication	Approval Status	Suggested Viscoelasticity Measurement Techniques
Approved products	Apligraf	Skin	Allogeneic fibroblasts in collagen matrix + allogeneic keratinocytes [viable]	Diabetic foot ulcers (DFU), venous leg ulcers (VLU)	FDA approval	AFM, Nanoindentation, OCE, Brillouin, Ultrasound Elastography, Passive Microrheology
	Dermagraft	Skin	Allogeneic fibroblasts seeded on polyglactin mesh scaffold [cryopreserved]	Diabetic foot ulcers	FDA approval	AFM, Nanoindentation, OCE, Brillouin, Ultrasound Elastography, Passive Microrheology
	Epicel	Skin	Autologous keratinocytes and murine cells (no material) [viable]	Large burns in adults and children	FDA approval 2016	AFM, Nanoindentation, OCE, Brillouin, Ultrasound Elastography, Passive Microrheology
	Gintuit	Skin	Allogeneic cultured keratinocytes and fibroblasts in bovine collagen	Dental applications	FDA approval	AFM, Nanoindentation, OCE, Brillouin, Ultrasound Elastography, Passive Microrheology
	Heart Sheet (Terumo)	Cardiac Tissue	Autologous skeletal myoblast cell sheet	Heart Failure	No US approval (sold in Japan)	AFM, Nanoindentation, OCE, Brillouin, Ultrasound Elastography, Passive Microrheology
	MACI	Cartilage	Autologous chondrocytes on collagen I/III membrane	Cartilage Repair	FDA approval	AFM, Nanoindentation, OCE, Brillouin, Ultrasound Elastography, Passive Microrheology
	Holocar [Europe]	Eyes	Autologous eye cells taken from patient biopsy cultured on fibrin matrix	Corneal Repair	EU approval	AFM, Nanoindentation, OCE, Brillouin, Ultrasound Elastography, Passive Microrheology
Commercial-backed Clinical Stage	Humacyte	Blood Vessel	Allogeneic aorta cells seeded on PGA mesh cultured under cyclic strain then decellularized	Vascular access/vascular grafts		AFM, Nanoindentation, OCE, Brillouin, Ultrasound Elastography, Passive Microrheology
	RVT-802	Lymph Nodes	Allogeneic decellularized thymus tissue (taken from other infants undergoing heart surgery)	Pediatric immunodeficiency		AFM, Nanoindentation, OCE, Brillouin, Ultrasound Elastography, Passive Microrheology
	Miromatrix	Liver, Kidney	Heavily involved in decellularization/recellularization protocols for liver, kidney tissues	Organ transplant	–	AFM, Nanoindentation, OCE, Brillouin, Ultrasound Elastography, Passive Microrheology
	Videregen	Lung	decellularization/recellularization processes for lung	Lung fistula	–	AFM, Nanoindentation, OCE,
	DeNovo Nt	Cartilage	Culture tissues for cartilage repair	Cartilage Repair		AFM, Nanoindentation, OCE, Brillouin, Ultrasound Elastography, Passive Microrheology
	Bioseed C	Cartilage	fibrin matrix seeded with chondrocytes (similar to MACI)	Cartilage Repair		AFM, Nanoindentation, OCE, Brillouin, Ultrasound Elastography, Passive Microrheology
	CaReS (Arthro-kinetics)	Cartilage	Chondrocytes cultured in collagen gel (34 mm diameter, 6–8 mm thick) and cultured for 12 days	Cartilage Repair		AFM, Nanoindentation, OCE, Ultrasound Elastography,
	Novocart 3D	Cartilage	Biphasic chondroitin sulfate-collagen scaffold seeded in vitro	Cartilage Repair	Phase 3 clinical trial in the US	AFM, Nanoindentation, OCE, Ultrasound Elastography,

tissue stiffness and viscoelastic characterization as part of manufacturing or product release assays. Therapies that aim to replace native tissues should match, or correlate to, the endogenous mechanical properties in a patient-specific manner to improve regenerative outcomes.[170,171] This goal would benefit from the nondestructive measurement of healthy host tissue and the batch-specific characterization of the engineered product to better match implants with the intended host; applicable measurement techniques, with a focus on those that preserve the sterility of the manufacturing process and that achieve measurements in a noninvasive or nondestructive manner, are mentioned below. Due to these criteria, many of the tools described here are expensive and nontrivial to operate, requiring technical expertise; these caveats pose a sizable barrier to the wide deployment of these tools for measuring biomaterial and tissue viscoelasticity immediately prior to patient implantation.

Articular cartilage is composed of a chondrocyte-laden extracellular matrix and plays a major role in movement by dissipating forces between joints. Specific organization of collagens and proteoglycans leads to a viscoelastic tissue that can resist compressive, tensile, and shear forces.[172] In the case of articular cartilage repair, implanted grafts must align with the mechanics of the surrounding tissue to enable proper regeneration.[170,171,173] Chondrocytes cultured on mechanically matching substrates, compared to native cartilage, have an enhanced cartilage-specific extracellular matrix.[171] In another study, strain compliance, and a stiffness lower than that of healthy tissue, led to improved regenerative outcomes.[170] AFM has been utilized to characterize multiscale stiffness and the friction coefficient to demonstrate the positive effect of mechanical conditioning on improving the quality of engineered cartilage implants.[173] In addition, viscoelastic properties of the cell's microenvironment can regulate their phenotype and change the secretion and organization of the cartilage extracellular matrix. Engineered cartilage hydrogels with high degrees of stress relaxation lead to increases in encapsulated cell collagen type II and aggrecan content as well as promote cell proliferation and survival.[174] Recently, the influence of implant viscoelasticity was evaluated with hyaluronic acid and alginate-based hydrogels with tunable mechanical properties, characterized via shear rheometry. This study demonstrated that an increase in hydrogel viscoelasticity led to enhanced chondrogenic cell phenotypes and improved glycosaminoglycan and collagen maturation within regenerated cartilage in vivo.[175] Currently, cartilage grafts are fabricated using a patient's own cells, which may vary widely patient-to-patient or be influenced by patient disease state. Different products are cultured for varying durations (days to weeks) before implantation and are not typically tested for their mechanical properties within standard lot release assays. Consideration of both graft stiffness as well as viscoelasticity relative to the patient's healthy cartilage may be important for improving therapeutic outcomes and increasing the chance of successful grafting.

Within the cardiovascular system, blood vessels are rich in collagens and elastin, which give rise to viscoelastic properties. The ability to dissipate circumferential forces along the vessel walls reduces fatigue, which is critical for long-term maintenance of function.[176] When occluded or blocked vessels need to be replaced, tissue-engineered vascular grafts represent a promising approach that reduces side effects compared to that of autologous implants.[177] The importance of matching

vascular graft mechanical properties for long-term vessel patency was identified over 40 years ago.[178,179] Therapeutic blood vessel implants, such as those in late-stage development by Humacyte, utilize an extended cell culture period prior to decellularization to generate vessel-specific extracellular matrix grafts. Mechanical properties of the graft upon implantation are critical, and retention strength, burst pressure, and percent compliance are commonly evaluated.[180] Dynamic mechanical analysis, among other techniques, can provide insight into vascular graft viscoelastic properties and be used to achieve more physiologically relevant engineered tissues.[181] With variations in cell source and patient valve mechanical properties, consideration of viscoelastic measurements for blood vessel grafts may provide useful insights for the in vitro maturation manufacturing step as well as improve patient-specific outcomes.

Heart valves are made up of interstitial cell-produced fibrillar collages, chondroitin sulfate proteoglycans, and elastin that give rise to its specific structure and mechanical properties.[182] Proper valve biomechanics are required to maintain the direction of blood flow. In conditions such as stenosis, stiffening of the valve prevents function, and the valve must be replaced. Biologic heart valve replacements are typically treated with glutaraldehyde, which significantly affects graft viscoelasticity.[183] This contrasts with the long-standing notion that valves demonstrate anisotropic viscoelastic behaviors critical to proper function and have been characterized using dynamic mechanical analysis[184] and modeled.[185] Interestingly, these studies highlight spatial differences in the viscoelastic properties of different regions within individual native valves. Again, considerations of native tissue properties, namely, coordinating valve viscoelasticity with healthy tissues, may improve therapeutic outcomes.

Among others, viscoelastic properties play important roles in other structural tissues, such as the meniscus.[186] In the nervous system, mechanical matching of implant to host minimizes foreign body reaction; stiffness above the native tissue threshold often precipitates a fibrotic response.[187]

4.2. Bioinks and 3D Bioprinting

Bioprinting respresents one exciting, emerging technology with numerous applications in the generation of functional tissue constructs to replace injured or diseased tissues. It offers high reproducibility and precise control over the fabricated constructs in an automated manner, potentially enabling high throughput production. During the bioprinting process, bioinks, which are solutions of biomaterials in the hydrogel that usually encapsulate the desired cell types, are used to print tissue constructs. These bioinks can be cross-linked or stabilized during or immediately after bioprinting to generate the final shape, structure, and architecture of the designed construct. Figure 29 reviews important characteristics of the bioinks. The mechanism and duration of cross-linking changes the viscoelasticity of the bioink. Bioinks may be made from natural or synthetic biomaterials alone, or a combination of the two as hybrid materials. An ideal bioink should possess proper mechanical, rheological, and biological properties of the target tissues, which are essential to ensure correct functionality of the bioprinted tissues and organs. The presence of strong viscoelastic character better supports vascularization[188] and enhances stem cell differentiation outcomes.[189] The most promising way to integrate stress relaxation properties to bioink formulations is to integrate physical or dynamic cross-
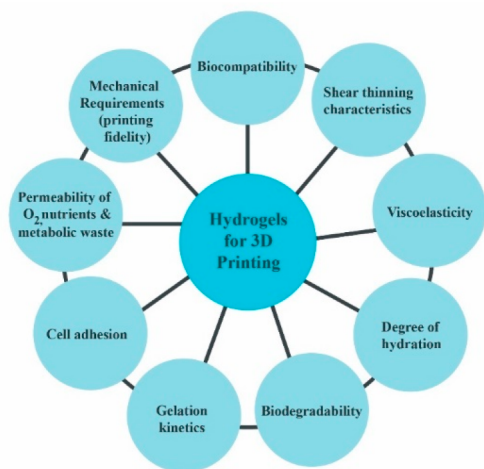
Figure 29. Some material properties that are critical for 3D printing.

links. These types of bonds can dissociate and reorganize under load[190] or be directly remodeled by pushing forces of embedded cells.[191] Interestingly, examples such as hydrazone chemistry also introduce pro-bioprinting characteristics of shear thinning and self-healing.[192] Even with these techniques, the ability to match the viscoelasticity of the tissue construct with that of the native host tissue remains a major challenge. Although noninvasive measurement probes permit more facile recording of bioink viscoelasticity, measuring the viscoelasticity of a hydrogel material is, in itself, very difficult due to the fluidity of the material. If the bioink includes live cells, nondestructive methods and probe sterility must also be considered. Overall, rigorous efforts should be adopted to ensure that target mechanical properties of the tissue constructs are achieved so as to maximize cell survivability and proper functionality after transplantation.[193]

4.3. In Vitro Models for Drug Development

2D cell cultures have been primarily used to study cell behaviors and their responses to drugs in the last 100 years. However, the cells' response to a drug in the body is very different than 2D cell culture platforms due to interaction of cells with other cells, the ECM, the effect of perfusion, and other chemical and mechanical stimuli in the 3D body that do not exist in 2D models. On the other hand, while animal models have contributed significantly both to our understanding of physiology and disease and to the development of new medicines, it has been known that animal testing is not a good predictor of human response to a drug. Some drug candidates may be terminated for lack of efficacy in animals or discovery of hazards or toxicity in animals that might not necessarily be relevant to humans. All these reasons give rise to a constant interest in the design of culture systems that can better sustain tissue functionality for extended times in vitro, which has led to the introduction of the microphysiological systems by NIH in 2011. The microphysiological systems are aimed to provide or support biochemical/electrical/mechanical responses to model a set of specific properties that define organ or tissue function. They are also called tissue chips and organs-on-a-chip. To improve biological mimicry, these organs-on-a-chip need 3D scaffolds to achieve 3D tissue constructs and include fluid flow for perfusion and experiencing shear stress. Each cell type requires a specific

viscoelastic property of the scaffold, which has led to the introduction of biomaterials with tunable viscoelasticity.

It is important to consider tissue-specific viscoelastic character, ranging from seconds in brain tissue to tens to hundreds of seconds for soft tissues such as muscle and skin.[44,60] Viscoelasticity is not only critical to establish representative tissue models,[194] but can also be indicative of age[195] or disease state.[196] In these studies, brain stiffness and viscoelasticity, typically measured with magnetic resonance elastography, decrease with disease progression and age.[197] Given methodological improvements in the generation of tissue-specific substrates with tunable stiffness and viscoelasticity, a worthy goal is not only the refinement of tissue-mimetics to encompass a variety of disease and age-specific mechanical characteristics, but also the generation of tissue substrates whose viscoelasticity is matched to the individual patient, thereby enabling a precision medicine approach to evaluating treatment efficacy. Finally, tools that enable the collection of a longitudinal record of time-varying changes in mechanical properties during treatment could furnish an informative supplement to standard biochemical measurements and potentially improve predictions of drug efficacy.

4.4. In Vitro Personalized Anticancer Drug Screening

One of the major benefits of in vitro drug screenings is the ability to evaluate over 100 types of anticancer drugs on the cells of a patient's own cells. However, these screenings cannot sufficiently and accurately predict the efficacy and toxicity of the drug without mimicking the tumor microenvironment, namely the dynamic viscoelastic properties.[198] It is essential to capture the biophysical conditions that tumors encounter during development and cancer progression, such as increases in tissue fluidity[191] or microenvironment stiffening[199] that have direct influence on tumor growth and metastasis. Inconsistent mechanical properties compared to native conditions can influence cell and tumor phenotype and subsequently negatively affect screening reliability. As this review has illustrated, the viscoelastic properties of the tumor environment result from the unique interaction between cancer cells, cancer-associated fibroblast cells, ECM, and vasculature. Moreover, it has been increasingly appreciated that modulating the tumor environment represents a druggable target for therapeutic intervention.[12] In one promising approach, researchers have developed new bioprinting techniques to not only print the cells within their ECM but also print vasculature networks.[200] In addition, tumor size can be controlled to obtain reliable and quantitative drug responses.[201] To develop cancer drug screening platforms, patient cancer cells (including associated fibroblasts and endothelial cells) can be derived from the biopsy sample and used to build a realistic model of the tumor in vitro. Importantly, the hydrogel substrate used for encapsulation must match the viscoelasticity of patient ECM[198] and also consider parameters of adhesivity and degradability[202] that have direct influence on cancer cell state. Thus, in the long term, being able to create 3D organoids that mimic the tumor environment would enable clinicians to screen a bank of candidate anticancer drugs to develop personalized cancer treatment regimens. Using the methodologies discussed in this review, tumor microenvironment viscoelasticity can be monitored over time as a predictive indicator for in vivo efficacy, since a stiffer microenvironment promotes metastasis and correlates with therapy resistive response.[203−206] Thus,

establishing and monitoring tumor microenvironment viscoelasticity in 3D in vitro models may improve functional screening to obtain the best possible clinical outcome for patients.

4.5. In Vitro Models for Precision Clinical Trials. In December 2022, a new legislation was signed into law by President Joe Biden that new medicines need not be tested in animals to receive U.S. Food and Drug Administration (FDA) approval. This will open a new era in clinical trials that uses organ-on-a-chip devices to replace animal testing. Organ-on-a-chip devices can recapitulate key functional aspects of tissues and organs. They use cell lines, primary cells, and induced pluripotent stem cells (iPS) to build a specific part of an organ. Each cell type requires its own scaffold with a specific range in viscoelasticity. Using patient-derived primary cells or iPS cells on the organ-on-a-chip devices creates a patient-on-a-chip model for testing drug toxicity and efficacy. So far 10 organ-on-a-chip have been linked to create body-on-a-chip to study drug pharmacokinetics and pharmacodynamics as a model for the whole body. It is anticipated that the use of these in vitro models increases significantly for precision medicine and precision clinical trials.[207−213] While still under development, awareness toward generating patient- and organ-specific viscoelasticity as well as measuring dynamic changes in viscoelasticity over time can provide valuable insights that are more challenging to obtain with traditional animal models.

5. FUTURE WORK

Of the aforementioned approaches for measuring viscoelasticity of biological samples, most require direct contact of the device with the sample. Herein, there has been intense interest to develop contactless methods, an endeavor that holds particular relevance for assaying viscoelasticity in fragile biomaterials or in cell culture and tissue specimens which would suffer irreparable damage or physical destruction by microbial contamination or direct probe contact, respectively. A few exciting examples of work within this arena at both the basic research and commercial level include: a contactless interfacial method to perform interfacial shear rheology on liquid/liquid interfaces using the broadly available imaging modality of confocal microscopy;[214] a colloidal-probe atomic force microscope for measuring the viscoelastic rheological properties of soft gels over a wide range of frequencies;[215] and a commercial tool (ElastoSens Bio)[82,83] for non-destructively measuring the viscoelastic properties of viscoelastic soft solids relevant to life science and biomedical research with repeatability and sensitivity. Other barriers to the widespread application of these tools for viscoelasticity measurement are their expense, their complexity in set-up and operation, and the technical expertise required for accurate data analysis and interpretation. More cost-effective, turn-key options are required in order to promote the widespread adoption of these methods for collecting viscoelasticity data in basic biological research as well as in the clinical setting. With respect to the latter, there is an urgent need to integrate rheological measurements with standard biological assessments, such as histopathology and patient health parameters from clinical evaluation, so as to instigate investigations into the bidirectional crosstalk between tissue biomechanics, biochemical processes, and gene regulatory events in health and in disease. In parallel with recent innovation in microfluidic platforms for profiling individual cells in multiomics,[216] advancements in platforms for nondestructive

sample (both cell- and tissue-level) handling and rheological characterization at the single-cell level will enable the productive integration of these technologies in the future for "multiomics+mechanical" studies. This may hold particular relevance for cancer biology, and degenerative diseases, where there remains tremendous unmet clinical need. Another foreseeable application of combining microfluidic with microrheology techniques is in cell sorting based on the viscoelasticity of cell organelles. It has been shown that high frequency microrheology can distinguish benign and malignant cancer cells.[217] At high frequency or short timescales, the dynamics of cell organelles emerge due to their short length-scale. Combining high frequency microrheology with flow cytometry can provide a high throughput method to examine changes in cell organelle mechanics to elucidate disease progression and response to therapies. Overall, the standardized collection of viscoelasticity datasets may augment our understanding of the multifaceted relationships between environmental mechanics, and tissue homeostasis, disease progression, and tissue regeneration at the resolution of single-cell trajectories.

■ CONCLUSION

We discussed the concept of viscoelasticity and its relevance to biomedical sciences. Several validated techniques for measuring viscoelasticity have been highlighted, and the accompanying comparison tables have been contructed with the explicit goal of helping biologists navigate how to apply the study of viscoelasticity to their own which method could best address their specific biomedical applications. Herein, recent technological advancements in viscoelasticity measurement techniques have greatly improved scientists' ability to characterize the mechanical properties of living tissues and of engineered biomaterials. These advancements are anticipated to drive discovery in several critical fields, from basic research and drug discovery in the R&D setting, to clinically-minded innovation in regenerative medicine and precision treatment of disease.

■ AUTHOR INFORMATION

Corresponding Author

Jennifer B. Treweek − *Department of Biomedical Engineering, University of Southern California, Los Angeles, California 90089, United States;* ● orcid.org/0000-0002-5601-9646; Email: jtreweek@usc.edu

Authors

Payam Eliahoo − *Department of Biomedical Engineering, University of Southern California, Los Angeles, California 90089, United States;* ● orcid.org/0000-0002-8269-1399

Hesam Setayesh − *Department of Biomedical Engineering, University of Southern California, Los Angeles, California 90089, United States*

Tyler Hoffman − *Department of Bioengineering, University of California Los Angeles, Los Angeles, California 90095, United States*

Yifan Wu − *Department of Bioengineering, University of California Los Angeles, Los Angeles, California 90095, United States*

Song Li − *Department of Bioengineering, University of California Los Angeles, Los Angeles, California 90095, United States;* ● orcid.org/0000-0002-4760-8828

Complete contact information is available at:

Author Contributions

The manuscript was written through contributions of all authors. All authors have given approval to the final version of the manuscript. CRediT: **Payam Eliahoo** writing-original draft, writing-review & editing; **Jennifer Brooke Treweek** conceptualization, funding acquisition, writing-original draft, writing-review & editing.

■ REFERENCES

(1) Hannezo, E.; Heisenberg, C. P. Mechanochemical Feedback Loops in Development and Disease. *Cell* **2019**, *178*, 12−25.

(2) Schiffhauer, E. S.; Robinson, D. N. Mechanochemical Signaling Directs Cell-Shape Change. *Biophys. J.* **2017**, *112*, 207−214.

(3) Scott, L. E.; Weinberg, S. H.; Lemmon, C. A. Mechanochemical Signaling of the Extracellular Matrix in Epithelial-Mesenchymal Transition. *Frontiers in Cell and Developmental Biology* **2019**, *7*, 135.

(4) Geng, J.; Kang, Z.; Sun, Q.; Zhang, M.; Wang, P.; Li, Y.; Li, J.; Su, B.; Wei, Q. Microtubule Assists Actomyosin to Regulate Cell Nuclear Mechanics and Chromatin Accessibility. *Research* **2023**, *6*, 0054.

(5) Park, J. S.; Burckhardt, C. J.; Lazcano, R.; Solis, L. M.; Isogai, T.; Li, L.; Chen, C. S.; Gao, B.; Minna, J. D.; Bachoo, R.; DeBerardinis, R. J.; Danuser, G. Mechanical Regulation of Glycolysis via Cytoskeleton Architecture. *Nature* **2020**, *578* (7796), 621−626.

(6) Romani, P.; Brian, I.; Santinon, G.; Pocaterra, A.; Audano, M.; Pedretti, S.; Mathieu, S.; Forcato, M.; Bicciato, S.; Manneville, J. B.; Mitro, N.; Dupont, S. Extracellular Matrix Mechanical Cues Regulate Lipid Metabolism through Lipin-1 and SREBP. *Nat. Cell Biol.* **2019**, *21* (3), 338−347.

(7) Gupta, V. K.; Chaudhuri, O. Mechanical Regulation of Cell-Cycle Progression and Division. *Trends in Cell Biology* **2022**, *32*, 773−785.

(8) Iyer, K. V.; Piscitello-Gómez, R.; Paijmans, J.; Jülicher, F.; Eaton, S. Epithelial Viscoelasticity Is Regulated by Mechanosensitive E-Cadherin Turnover. *Curr. Biol.* **2019**, *29* (4), 578−591.

(9) Zhou, C.; Zhang, D.; Du, W.; Zou, J.; Li, X.; Xie, J. Substrate Mechanics Dictate Cell-Cell Communication by Gap Junctions in Stem Cells from Human Apical Papilla. *Acta Biomater* **2020**, *107*, 178−193.

(10) Heisenberg, C. P.; Bellaïche, Y. XForces in Tissue Morphogenesis and Patterning. *Cell* **2013**, *153*, 948.

(11) Piersma, B.; Hayward, M. K.; Weaver, V. M. Fibrosis and Cancer: A Strained Relationship. *Biochim Biophys Acta Rev. Cancer* **2020**, *1873* (2), 188356.

(12) Sahai, E.; Astsaturov, I.; Cukierman, E.; DeNardo, D. G.; Egeblad, M.; Evans, R. M.; Fearon, D.; Greten, F. R.; Hingorani, S. R.; Hunter, T.; Hynes, R. O.; Jain, R. K.; Janowitz, T.; Jorgensen, C.; Kimmelman, A. C.; Kolonin, M. G.; Maki, R. G.; Powers, R. S.; Puré, E.; Ramirez, D. C.; Scherz-Shouval, R.; Sherman, M. H.; Stewart, S.; Tlsty, T. D.; Tuveson, D. A.; Watt, F. M.; Weaver, V.; Weeraratna, A. T.; Werb, Z. A Framework for Advancing Our Understanding of Cancer-Associated Fibroblasts. *Nat. Rev. Cancer* **2020**, *20* (3), 174−186.

(13) Wu, P.-H.; Aroush, D. R.-B.; Asnacios, A.; Chen, W.-C.; Dokukin, M. E.; Doss, B. L.; Durand-Smet, P.; Ekpenyong, A.; Guck, J.; Guz, N. V.; Janmey, P. A.; Lee, J. S. H.; Moore, N. M.; Ott, A.; Poh,

Y.-C.; Ros, R.; Sander, M.; Sokolov, I.; Staunton, J. R.; Wang, N.; Whyte, G.; Wirtz, D. A Comparison of Methods to Assess Cell Mechanical Properties. *Nat. Methods* **2018**, *15* (7), 491−498.

(14) Henke, E.; Nandigama, R.; Ergün, S. Extracellular Matrix in the Tumor Microenvironment and Its Impact on Cancer Therapy. *Frontiers in Molecular Biosciences* **2020**, *6*, 160.

(15) Xu, S.; Xu, H.; Wang, W.; Li, S.; Li, H.; Li, T.; Zhang, W.; Yu, X.; Liu, L. The Role of Collagen in Cancer: From Bench to Bedside. *Journal of Translational Medicine* **2019**, *17* (1), 1.

(16) Jiang, Y.; Zhang, H.; Wang, J.; Liu, Y.; Luo, T.; Hua, H. Targeting Extracellular Matrix Stiffness and Mechanotransducers to Improve Cancer Therapy. *Journal of Hematology and Oncology* **2022**, *15* (1), 34.

(17) Caragine, C. M.; Kanellakopoulos, N.; Zidovska, A. Mechanical Stress Affects Dynamics and Rheology of the Human Genome. *Soft Matter* **2021**, *18* (1), 107−116.

(18) Wintner, O.; Hirsch-Attas, N.; Schlossberg, M.; Brofman, F.; Friedman, R.; Kupervaser, M.; Kitsberg, D.; Buxboim, A. A Unified Linear Viscoelastic Model of the Cell Nucleus Defines the Mechanical Contributions of Lamins and Chromatin. *Advanced Science* **2020**, *7* (8), 1901222.

(19) Basic Elasticity and Viscoelasticity. *J. Conserv Dent*. Princeton University Press, 2008, Vol. *11*, pp 37−41.

(20) Rus, G.; Faris, I. H.; Torres, J.; Callejas, A.; Melchor, J. Why Are Viscosity and Nonlinearity Bound to Make an Impact in Clinical Elastographic Diagnosis? *Sensors* **2020**, *20* (8), 2379.

(21) Saraswathibhatla, A.; Indana, D.; Chaudhuri, O. Cell-Extracellular Matrix Mechanotransduction in 3D. *Nature Reviews Molecular Cell Biology* **2023**, *24*, 495−516.

(22) Janmey, P. A.; Fletcher, D. A.; Reinhart-King, C. A. Stiffness Sensing by Cells. *Physiol Rev.* **2020**, *100* (2), 695−724.

(23) Uhler, C.; Shivashankar, G. V. Regulation of Genome Organization and Gene Expression by Nuclear Mechanotransduction. *Nature Reviews Molecular Cell Biology* **2017**, *18*, 717−727.

(24) Iskratsch, T.; Wolfenson, H.; Sheetz, M. P. Appreciating Force and Shape-the Rise of Mechanotransduction in Cell Biology. *Nature Reviews Molecular Cell Biology* **2014**, *15*, 825−833.

(25) Ursini-Siegel, J. *Tumor Micro-Environment Methods and Protocols*, 2nd Ed.; Springer Nature, Methods in Molecular Biology, Vol. *2614*, 2023. http://www.springer.com/series/7651.

(26) Seo, B. R.; Chen, X.; Ling, L.; Song, Y. H.; Shimpi, A. A.; Choi, S.; Gonzalez, J.; Sapudom, J.; Wang, K.; Andresen Eguiluz, R. C.; Gourdon, D.; Shenoy, V. B.; Fischbach, C. Collagen Microarchitecture Mechanically Controls Myofibroblast Differentiation. *Proc. Natl. Acad. Sci. U.S.A.* **2020**, *117*, 11387.

(27) Risom, T.; Glass, D. R.; Averbukh, I.; Liu, C. C.; Baranski, A.; Kagel, A.; McCaffrey, E. F.; Greenwald, N. F.; Rivero-Gutiérrez, B.; Strand, S. H.; Varma, S.; Kong, A.; Keren, L.; Srivastava, S.; Zhu, C.; Khair, Z.; Veis, D. J.; Deschryver, K.; Vennam, S.; Maley, C.; Hwang, E. S.; Marks, J. R.; Bendall, S. C.; Colditz, G. A.; West, R. B.; Angelo, M. Transition to Invasive Breast Cancer Is Associated with Progressive Changes in the Structure and Composition of Tumor Stroma. *Cell* **2022**, *185* (2), 299−310.

(28) Liu, Y.; Galior, K.; Ma, V. P. Y.; Salaita, K. Molecular Tension Probes for Imaging Forces at the Cell Surface. *Acc. Chem. Res.* **2017**, *50* (12), 2915−2924.

(29) Kaur, A.; Ecker, B. L.; Douglass, S. M.; Kugel, C. H.; Webster, M. R.; Almeida, F. V.; Somasundaram, R.; Hayden, J.; Ban, E.; Ahmadzadeh, H.; Franco-Barraza, J.; Shah, N.; Mellis, I. A.; Keeney, F.; Kossenkov, A.; Tang, H. Y.; Yin, X.; Liu, Q.; Xu, X.; Fane, M.; Brafford, P.; Herlyn, M.; Speicher, D. W.; Wargo, J. A.; Tetzlaff, M. T.; Haydu, L. E.; Raj, A.; Shenoy, V.; Cukierman, E.; Weeraratna, A. T. Remodeling of the Collagen Matrix in Aging Skin Promotes Melanoma Metastasis and Affects Immune Cell Motility. *Cancer Discov* **2019**, *9* (1), 64−81.

(30) Polacheck, W. J.; Chen, C. S. Measuring Cell-Generated Forces: A Guide to the Available Tools. *Nature Methods* **2016**, *13*, 415−423.

(31) Kai, F.; Ou, G.; Tourdot, R. W.; Stashko, C.; Gaietta, G.; Swift, M. F.; Volkmann, N.; Long, A. F.; Han, Y.; Huang, H. H.; Northey, J. J.; Leidal, A. M.; Viasnoff, V.; Bryant, D. M.; Guo, W.; Wiita, A. P.; Guo, M.; Dumont, S.; Hanein, D.; Radhakrishnan, R.; Weaver, V. M. ECM Dimensionality Tunes Actin Tension to Modulate Endoplasmic Reticulum Function and Spheroid Phenotypes of Mammary Epithelial Cells. *EMBO J.* **2022**, *41* (17), e109205.

(32) Furman, S. *Effects of Stiffness and Cell Shape on Cellular Mechanosensing*; Master's thesis; Rowan University: Glassboro, NJ, USA, 2021.

(33) Hayward, M. K.; Muncie, J. M.; Weaver, V. M. Tissue Mechanics in Stem Cell Fate, Development, and Cancer. *Developmental Cell* **2021**, *56*, 1833−1847.

(34) Ge, H.; Tian, M.; Pei, Q.; Tan, F.; Pei, H. Extracellular Matrix Stiffness: New Areas Affecting Cell Metabolism. *Frontiers in Oncology* **2021**, *11*, 631991.

(35) Kaur, A.; Ecker, B. L.; Douglass, S. M.; Kugel, C. H.; Webster, M. R.; Almeida, F. v.; Somasundaram, R.; Hayden, J.; Ban, E.; Ahmadzadeh, H.; Franco-Barraza, J.; Shah, N.; Mellis, I. A.; Keeney, F.; Kossenkov, A.; Tang, H. Y.; Yin, X.; Liu, Q.; Xu, X.; Fane, M.; Brafford, P.; Herlyn, M.; Speicher, D. W.; Wargo, J. A.; Tetzlaff, M. T.; Haydu, L. E.; Raj, A.; Shenoy, V.; Cukierman, E.; Weeraratna, A. T. Remodeling of the Collagen Matrix in Aging Skin Promotes Melanoma Metastasis and Affects Immune Cell Motility. *Cancer Discov* **2019**, *9* (1), 64−81.

(36) Pegoraro, A. F.; Janmey, P.; Weitz, D. A. Mechanical Properties of the Cytoskeleton and Cells. *Cold Spring Harb Perspect Biol.* **2017**, *9* (11), a022038.

(37) Martino, F.; Perestrelo, A. R.; Vinarský, V.; Pagliari, S.; Forte, G. Cellular Mechanotransduction: From Tension to Function. *Frontiers in Physiology* **2018**, *9*, 00824.

(38) Song, Y.; Soto, J.; Chen, B.; Hoffman, T.; Zhao, W.; Zhu, N.; Peng, Q.; Liu, L.; Ly, C.; Wong, P. K.; Wang, Y.; Rowat, A. C.; Kurdistani, S. K.; Li, S. Transient Nuclear Deformation Primes Epigenetic State and Promotes Cell Reprogramming. *Nat. Mater.* **2022**, *21* (10), 1191−1199.

(39) Pittman, M.; Iu, E.; Li, K.; Wang, M.; Chen, J.; Taneja, N.; Jo, M. H.; Park, S.; Jung, W. H.; Liang, L.; Barman, I.; Ha, T.; Gaitanaros, S.; Liu, J.; Burnette, D.; Plotnikov, S.; Chen, Y. Membrane Ruffling Is a Mechanosensor of Extracellular Fluid Viscosity. *Nat. Phys.* **2022**, *18* (9), 1112−1121.

(40) Romani, P.; Valcarcel-Jimenez, L.; Frezza, C.; Dupont, S. Crosstalk between Mechanotransduction and Metabolism. *Nature Reviews Molecular Cell Biology* **2021**, *22*, 22−38.

(41) Park, S.; Koch, D.; Cardenas, R.; Kas, J.; Shih, C.K. Cell Motility and Local Viscoelasticity of Fibroblasts. *Biophys. J.* **2005**, *89* (6), 4330−4342.

(42) Humphrey, J. D.; Dufresne, E. R.; Schwartz, M. A. Mechanotransduction and Extracellular Matrix Homeostasis. *Nature Reviews Molecular Cell Biology* **2014**, *15*, 802−812.

(43) Bonnans, C.; Chou, J.; Werb, Z. Remodelling the Extracellular Matrix in Development and Disease. *Nature Reviews Molecular Cell Biology* **2014**, *15*, 786−801.

(44) Chaudhuri, O.; Cooper-White, J.; Janmey, P. A.; Mooney, D. J.; Shenoy, V. B. Effects of Extracellular Matrix Viscoelasticity on Cellular Behaviour. *Nature* **2020**, *584* (7822), 535−546.

(45) Winkler, J.; Abisoye-Ogunniyan, A.; Metcalf, K. J.; Werb, Z. Concepts of Extracellular Matrix Remodelling in Tumour Progression and Metastasis. *Nature Communications* **2020**, *11*, 1.

(46) Wolfenson, H.; Yang, B.; Sheetz, M. P. Annual Review of Physiology Steps in Mechanotransduction Pathways That Control Cell Morphology. *Annu. Rev. Physiol.* **2019**, *81*, 585.

(47) Yeung, T.; Georges, P. C.; Flanagan, L. A.; Marg, B.; Ortiz, M.; Funaki, M.; Zahir, N.; Ming, W.; Weaver, V.; Janmey, P. A. Effects of Substrate Stiffness on Cell Morphology, Cytoskeletal Structure, and Adhesion. *Cell Motil Cytoskeleton* **2005**, *60* (1), 24−34.

(48) Bangasser, B. L.; Shamsan, G. A.; Chan, C. E.; Opoku, K. N.; Tüzel, E.; Schlichtmann, B. W.; Kasim, J. A.; Fuller, B. J.;

(49) McCullough, B. R.; Rosenfeld, S. S.; Odde, D. J. Shifting the Optimal Stiffness for Cell Migration. *Nat. Commun.* **2017**, *8*, 15313.

(49) Engler, A. J.; Sen, S.; Sweeney, H. L.; Discher, D. E. Matrix Elasticity Directs Stem Cell Lineage Specification. *Cell* **2006**, *126* (4), 677−689.

(50) Trappmann, B.; Gautrot, J. E.; Connelly, J. T.; Strange, D. G. T.; Li, Y.; Oyen, M. L.; Cohen Stuart, M. A.; Boehm, H.; Li, B.; Vogel, V.; Spatz, J. P.; Watt, F. M.; Huck, W. T. S. Extracellular-Matrix Tethering Regulates Stem-Cell Fate. *Nat. Mater.* **2012**, *11* (7), 642−649.

(51) Engler, A. J.; Griffin, M. A.; Sen, S.; Bönnemann, C. G.; Sweeney, H. L.; Discher, D. E. Myotubes Differentiate Optimally on Substrates with Tissue-like Stiffness: Pathological Implications for Soft or Stiff Microenvironments. *J. Cell Biol.* **2004**, *166* (6), 877−887.

(52) Baker, B. M.; Trappmann, B.; Wang, W. Y.; Sakar, M. S.; Kim, I. L.; Shenoy, V. B.; Burdick, J. A.; Chen, C. S. Cell-Mediated Fibre Recruitment Drives Extracellular Matrix Mechanosensing in Engineered Fibrillar Microenvironments. *Nat. Mater.* **2015**, *14* (12), 1262−1268.

(53) Segel, M.; Neumann, B.; Hill, M. F. E.; Weber, I. P.; Viscomi, C.; Zhao, C.; Young, A.; Agley, C. C.; Thompson, A. J.; Gonzalez, G. A.; Sharma, A.; Holmqvist, S.; Rowitch, D. H.; Franze, K.; Franklin, R. J. M.; Chalut, K. J. Niche Stiffness Underlies the Ageing of Central Nervous System Progenitor Cells. *Nature* **2019**, *573* (7772), 130−134.

(54) Shin, J. W.; Mooney, D. J. Extracellular Matrix Stiffness Causes Systematic Variations in Proliferation and Chemosensitivity in Myeloid Leukemias. *Proc. Natl. Acad. Sci. U. S. A.* **2016**, *113* (43), 12126−12131.

(55) Chaudhuri, O.; Gu, L.; Darnell, M.; Klumpers, D.; Bencherif, S. A.; Weaver, J. C.; Huebsch, N.; Mooney, D. J. Substrate Stress Relaxation Regulates Cell Spreading. *Nat. Commun.* **2015**, *6*, 7365.

(56) Chaudhuri, O.; Gu, L.; Klumpers, D.; Darnell, M.; Bencherif, S. A.; Weaver, J. C.; Huebsch, N.; Lee, H. P.; Lippens, E.; Duda, G. N.; Mooney, D. J. Hydrogels with Tunable Stress Relaxation Regulate Stem Cell Fate and Activity. *Nat. Mater.* **2016**, *15* (3), 326−334.

(57) Lee, H. P.; Gu, L.; Mooney, D. J.; Levenston, M. E.; Chaudhuri, O. Mechanical Confinement Regulates Cartilage Matrix Formation by Chondrocytes. *Nat. Mater.* **2017**, *16* (12), 1243−1251.

(58) Adebowale, K.; Gong, Z.; Hou, J. C.; Wisdom, K. M.; Garbett, D.; Lee, H.-p.; Nam, S.; Meyer, T.; Odde, D. J.; Shenoy, V. B.; Chaudhuri, O. Enhanced Substrate Stress Relaxation Promotes Filopodia-Mediated Cell Migration. *Nat. Mater.* **2021**, *20* (9), 1290−1299.

(59) Wei, Z.; Schnellmann, R.; Pruitt, H. C.; Gerecht, S. Hydrogel Network Dynamics Regulate Vascular Morphogenesis. *Cell Stem Cell* **2020**, *27* (5), 798−812.

(60) Elosegui-Artola, A.; Gupta, A.; Najibi, A. J.; Seo, B. R.; Garry, R.; Tringides, C. M.; de Lázaro, I.; Darnell, M.; Gu, W.; Zhou, Q.; Weitz, D. A.; Mahadevan, L.; Mooney, D. J. Matrix Viscoelasticity Controls Spatiotemporal Tissue Organization. *Nat. Mater.* **2023**, *22* (1), 117−127.

(61) Krajina, B. A.; Lesavage, B. L.; Roth, J. G.; Zhu, A. W.; Cai, P. C.; Spakowitz, A. J.; Heilshorn, S. C. Microrheology Reveals Simultaneous Cell-Mediated Matrix Stiffening and Fluidization That Underlie Breast Cancer Invasion. *Sci Adv* **2021**, *7* (8), eabe1969.

(62) Schramm, G. *A Practical Approach to Rheology and Rheometry*; Thermo Electron (Karlsruhe) GmbH, 2nd ed., 2004. www.thermo.com/mc.

(63) Ewoldt, R. H.; Johnston, M. T.; Caretta, L. M. *Experimental Challenges of Shear Rheology: How to Avoid Bad Data* **2015**, 207−241.

(64) Giessibl, F. J. Advances in Atomic Force Microscopy. *REVIEWS OF MODERN PHYSICS* **2003**, *75*, 949.

(65) Nandi, T.; Ainavarapu, S. R. K. Applications of Atomic Force Microscopy in Modern Biology. *Emerging Topics in Life Sciences* **2021**, *5*, 103−111.

(66) Krieg, M.; Fläschner, G.; Alsteens, D.; Gaub, B. M.; Roos, W. H.; Wuite, G. J. L.; Gaub, H. E.; Gerber, C.; Dufrêne, Y. F.; Müller, D.

J. Atomic Force Microscopy-Based Mechanobiology. *Nature Reviews Physics* **2019**, *1*, 41−57.

(67) Deng, X.; Xiong, F.; Li, X.; Xiang, B.; Li, Z.; Wu, X.; Guo, C.; Li, X.; Li, Y.; Li, G.; Xiong, W.; Zeng, Z. Application of Atomic Force Microscopy in Cancer Research. *Journal of Nanobiotechnology* **2018**, *16*, 1.

(68) Gupta, S. Review on Atomic Force Microscopy. *Journal of Emerging Technologies and Innovative Research* **2019**, *6* (2), 508.

(69) Deng, X.; Xiong, F.; Li, X.; Xiang, B.; Li, Z.; Wu, X.; Guo, C.; Li, X.; Li, Y.; Li, G.; Xiong, W.; Zeng, Z. Application of Atomic Force Microscopy in Cancer Research. *Journal of Nanobiotechnology* **2018**, *16*, 1.

(70) Müller, D. J.; Dumitru, A. C.; lo Giudice, C.; Gaub, H. E.; Hinterdorfer, P.; Hummer, G.; de Yoreo, J. J.; Dufrêne, Y. F.; Alsteens, D. Atomic Force Microscopy-Based Force Spectroscopy and Multiparametric Imaging of Biomolecular and Cellular Systems. *Chemical Reviews* **2021**, *121*, 11701−11725.

(71) Patel, A. N.; Kranz, C. (Multi)Functional Atomic Force Microscopy Imaging. *Annual Rev. Anal. Chem.* **2018**, *11*, 329.

(72) Ando, T. High-Speed Atomic Force Microscopy and Its Future Prospects. *Biophysical Reviews* **2018**, *10*, 285−292.

(73) Vahabi, S.; Nazemi Salman, B.; Javanmard, A. Atomic Force Microscopy Application in Biological Research: A Review Study. *Iran J Med Sci.* **2013**, *38* (2), 76−83.

(74) Cao, D.; Song, Y.; Peng, J.; Ma, R.; Guo, J.; Chen, J.; Li, X.; Jiang, Y.; Wang, E.; Xu, L. Advances in Atomic Force Microscopy: Weakly Perturbative Imaging of the Interfacial Water. *Front Chem.* **2019**, *7*, 00626.

(75) Dufrêne, Y. F.; Ando, T.; Garcia, R.; Alsteens, D.; Martinez-Martin, D.; Engel, A.; Gerber, C.; Müller, D. J. Imaging Modes of Atomic Force Microscopy for Application in Molecular and Cell Biology. *Nature Nanotechnology* **2017**, *12*, 295−307.

(76) Chen, J.; Xu, K. Applications of Atomic Force Microscopy in Materials, Semiconductors, Polymers, and Medicine: A Minireview. *Instrumentation Science and Technology* **2020**, *48*, 667−681.

(77) Atomic Force Microscopy Market Size, Share, and Industry Analysis and Market Forecast to 2024. *MarketsandMarkets*. https://www.marketsandmarkets.com/Market-Reports/atomic-force-microscopy-market-57704156.html?gclid=EAIaIQobChMI6aiqhfqH6wIVvh-tBh2BxAkxEAAYASAAEgJmB_D_BwE (accessed 2020−08−05).

(78) Patel, A. N.; Kranz, C. Annual Review of Analytical Chemistry (Multi)Functional Atomic Force Microscopy Imaging. *Annual Review of Analytical Chemistry* **2018**, *11*, 329.

(79) Mann, A. B. Chapter 9: Nanoindentation. *Surfaces and Interfaces for Biomaterials*. Pankaj, V., Ed.; Woodhead Publishing, 2005, pp 225−247, ISBN 9781855739307, . https://www.sciencedirect.com/science/article/pii/B9781855739307500091.

(80) Mark, R. VanLandingham. *Review of Instrumented Indentation* **2003**, *108* (4), 20899−8610.

(81) Chavan, D.; Van De Watering, T. C.; Gruca, G.; Rector, J. H.; Heeck, K.; Slaman, M.; Iannuzzi, D. Ferrule-Top Nanoindenter: An Optomechanical Fiber Sensor for Nanoindentation. *Rev. Sci. Instrum.* **2012**, *83* (11), 1.

(82) *Soft Materials Testing Instruments I. Rheolution Inc.* https://www.rheolution.com/ (accessed 2020−08−08).

(83) Ceccaldi, C.; Strandman, S.; Hui, E.; Montagnon, E.; Schmitt, C.; Hadj Henni, A.; Lerouge, S. Validation and Application of a Nondestructive and Contactless Method for Rheological Evaluation of Biomaterials. *J. Biomed Mater. Res. B Appl. Biomater* **2017**, *105* (8), 2565−2573.

(84) Larin, K. V.; Scarcelli, G.; Yakovlev, V. V. Optical Elastography and Tissue Biomechanics. *J. Biomed Opt* **2019**, *24* (11), 1.

(85) Kennedy, B. F.; Wijesinghe, P.; Sampson, D. D. The Emergence of Optical Elastography in Biomedicine. *Nat. Photonics* **2017**, *11* (4), 215−221.

(86) *CSS450: Optical Rheology Systems : Quote, RFQ, Price and Buy.* https://www.azom.com/equipment-details.aspx?EquipID=6701 (accessed 2021−12−19).

(87) Robertson-Anderson, R. M. Optical Tweezers Microrheology: From the Basics to Advanced Techniques and Applications. *ACS Macro Lett.* **2018**, *7* (8), 968−975.

(88) Wang, S.; Larin, K. V. Optical Coherence Elastography for Tissue Characterization: A Review. *Journal of Biophotonics* **2015**, 279−302.

(89) Mohan, A. Mechanical and Novel Optical Techniques for Rheological Characterisation of Cereal Beta-Glucan. *International Journal of ChemTech Research* **2014**, *6* (5), 2732−2738.

(90) Walsh, A. J.; Cook, R. S.; Sanders, M. E.; Aurisicchio, L.; Ciliberto, G.; Arteaga, C. L.; Skala, M. C. Quantitative Optical Imaging of Primary Tumor Organoid Metabolism Predicts Drug Response in Breast Cancer. *Cancer Res.* **2014**, *74* (18), 5184−5194.

(91) Liu, H.-C.; Kijanka, P.; Urban, M. W. Four-Dimensional (4D) Phase Velocity Optical Coherence Elastography in Heterogeneous Materials and Biological Tissue. *Biomed Opt Express* **2020**, *11* (7), 3795.

(92) Tschöpe, A.; Birster, K.; Trapp, B.; Bender, P.; Birringer, R. Nanoscale Rheometry of Viscoelastic Soft Matter by Oscillating Field Magneto-Optical Transmission Using Ferromagnetic Nanorod Colloidal Probes. *J. Appl. Phys.* **2014**, *116* (18), 1.

(93) Liu, H. C.; Kijanka, P.; Urban, M. W. Acoustic Radiation Force Optical Coherence Elastography for Evaluating Mechanical Properties of Soft Condensed Matters and Its Biological Applications. *J. Biophotonics* **2020**, *13* (3), 1.

(94) Taylor, M. A.; Kijas, A. W.; Wang, Z.; Lauko, J.; Rowan, A. E. Heterodyne Brillouin Microscopy for Biomechanical Imaging. *Biomed Opt Express* **2021**, *12* (10), 6259.

(95) Troyanova-Wood, M.; Yakovlev, V. Multi-Wavelength Excitation Brillouin Spectroscopy. *IEEE J. Sel. Top. Quantum Electron.* **2021**, *27* (4), 1.

(96) Yun, S. H.; Chernyak, D. Brillouin Microscopy: Assessing Ocular Tissue Biomechanics. *Current Opinion in Ophthalmology* **2018**, 299−305.

(97) Prevedel, R.; Diz-Muñoz, A.; Ruocco, G.; Antonacci, G. Brillouin Microscopy: An Emerging Tool for Mechanobiology. *Nature Methods* **2019**, 969−977.

(98) Prevedel, R.; Diz-Muñoz, A.; Ruocco, G.; Antonacci, G. Brillouin Microscopy-a Revolutionary Tool for Mechanobiology? *arXivLabs*. Cornell University, arXiv:1901.02006v1 [physics.bio-ph], 2019. . (Accessed 2022−11−28.)

(99) Meng, Z.; Baker, R.; Panin, V. M.; Yakovlev, V. V. Brillouin Spectroscopy Reveals Changes in Muscular Viscoelasticity in Drosophila POMT Mutants. *Optical Elastography and Tissue Biomechanics II* **2015**, *9327*, 932713.

(100) Antonacci, G.; Beck, T.; Bilenca, A.; Czarske, J.; Elsayad, K.; Guck, J.; Kim, K.; Krug, B.; Palombo, F.; Prevedel, R.; Scarcelli, G. Recent Progress and Current Opinions in Brillouin Microscopy for Life Science Applications. *Biophys Rev* **2020**, *12*, 615−624.

(101) *Brillouin Microscopy—Measuring Mechanics in Biology Using Light Introduction—Why Mechanics Matters in Biology*. infocus Magazine, (53) **2019**. .

(102) Bevilacqua, C.; Gomez, J. M.; Fiuza, U.-M.; Chan, C. J.; Wang, L.; Hambura, S.; Eguren, M.; Ellenberg, J.; Diz-Munoz, A.; Leptin, M.; Prevedel, R. High-Resolution Line-Scan Brillouin Microscopy for Live-Imaging of Mechanical Properties during Embryo Development. *Nat. Methods* **2023**, *20*, 755−760.

(103) Bhatia, S. N.; Ingber, D. E. Microfluidic Organs-on-Chips. *Nat. Biotechnol.* **2014**, *32*, 760−772.

(104) Pipe, C. J.; McKinley, G. H. Microfluidic Rheometry. *Mech Res. Commun.* **2009**, *36* (1), 110−120.

(105) Urbanska, M.; Muñoz, H. E.; Shaw Bagnall, J.; Otto, O.; Manalis, S. R.; Di Carlo, D.; Guck, J. A Comparison of Microfluidic Methods for High-Throughput Cell Deformability Measurements. *Nat. Methods* **2020**, *17* (6), 587−593.

(106) Wang, H.; Liu, Z.; Shin, D. M.; Chen, Z. G.; Cho, Y.; Kim, Y. J.; Han, A. A Continuous-Flow Acoustofluidic Cytometer for Single-Cell Mechanotyping. *Lab Chip* **2019**, *19* (3), 387−393.

(107) Zhao, W.; Wang, H.; Guo, Y.; Sun, K.; Cheng, Z.; Chen, H. A High-Throughput Label-Free Time-Stretch Acoustofluidic Imaging Cytometer for Single-Cell Mechanotyping. *Microfluid Nanofluidics* **2020**, *24* (11), 1.

(108) González-Bermúdez, B.; Guinea, G. V.; Plaza, G. R. Advances in Micropipette Aspiration: Applications in Cell Biomechanics, Models, and Extended Studies. *Biophys. J.* **2019**, *116*, 587−594.

(109) Guevorkian, K.; Maître, J. L. Micropipette Aspiration: A Unique Tool for Exploring Cell and Tissue Mechanics in Vivo. *Methods Cell Biol.* **2017**, *139*, 187−201.

(110) Du, Y.; Zhang, S.; Cheng, D.; Liu, Y.; Sun, M.; Zhao, Q.; Cui, M.; Zhao, X. The Full Model of Micropipette Aspiration of Cells: A Mesoscopic Simulation. *Acta Biomater* **2023**, *157*, 297.

(111) Micklavzina, B. L.; Luferov, K.; Longo, M. L. Rheological Characterization of Mixed Surfactant Films at Droplet Interfaces via Micropipette Aspiration. *Langmuir* **2018**, *34* (29), 8560−8570.

(112) Daza, R.; González-Bermúdez, B.; Cruces, J.; De la Fuente, M.; Plaza, G. R.; Arroyo-Hernández, M.; Elices, M.; Pérez-Rigueiro, J.; Guinea, G. V. Comparison of Cell Mechanical Measurements Provided by Atomic Force Microscopy (AFM) and Micropipette Aspiration (MPA). *J. Mech Behav Biomed Mater.* **2019**, *95*, 103−115.

(113) Tabatabaei, M.; Tafazzoli-Shadpour, M.; Khani, M. M. Altered Mechanical Properties of Actin Fibers Due to Breast Cancer Invasion: Parameter Identification Based on Micropipette Aspiration and Multiscale Tensegrity Modeling. *Med. Biol. Eng. Comput* **2021**, *59*, 547−560.

(114) Berardi, M.; Bielawski, K.; Rijnveld, N.; Gruca, G.; Aardema, H.; van Tol, L.; Wuite, G.; Akca, B. I. Optical Interferometry Based Micropipette Aspiration Provides Real-Time Sub-Nanometer Spatial Resolution. *Commun. Biol.* **2021**, *4* (1), 1.

(115) Pelipenko, J.; Kristl, J.; Rošic, R.; Baumgartner, S.; Kocbek, P. Interfacial Rheology: An Overview of Measuring Techniques and Its Role in Dispersions and Electrospinning. *Acta Pharmaceutica.* **2012**, *62*, 123−140.

(116) El Omari, Y.; Yousfi, M.; Duchet-Rumeau, J.; Maazouz, A. Recent Advances in the Interfacial Shear and Dilational Rheology of Polymer Systems: From Fundamentals to Applications. *Polymers* **2022**, *14*, 2844.

(117) Brooks, C. F.; Fuller, G. G.; Frank, C. W.; Robertson, C. R. Interfacial Stress Rheometer to Study Rheological Transitions in Monolayers at the Air-Water Interface. *Langmuir* **1999**, *15* (7), 2450−2459.

(118) Kondej, D.; Sosnowski, T. R. Interfacial Rheology for the Assessment of Potential Health Effects of Inhaled Carbon Nanomaterials at Variable Breathing Conditions. *Sci. Rep* **2020**, *10* (1), 1.

(119) Anseth, J. W.; Goffin, A. J.; Fuller, G. G.; Ghio, A. J.; Kao, P. N.; Upadhyay, D. Lung Surfactant Gelation Induced by Epithelial Cells Exposed to Air Pollution or Oxidative Stress. *Am. J. Respir. Cell Mol. Biol.* **2005**, *33* (2), 161−168.

(120) Svitova, T. F.; Lin, M. C. Tear Lipids Interfacial Rheology: Effect of Lysozyme and Lens Care Solutions. *Optometry and Vision Science* **2010**, *87* (1), 10−20.

(121) Ariola, F. S.; Krishnan, A.; Vogler, E. A. Interfacial Rheology of Blood Proteins Adsorbed to the Aqueous-Buffer/Air Interface. *Biomaterials* **2006**, *27* (18), 3404−3412.

(122) Lhermerout, R.; Perrin, H.; Rolley, E.; Andreotti, B.; Davitt, K. A Moving Contact Line as a Rheometer for Nanometric Interfacial Layers. *Nat. Commun.* **2016**, *7*, 1.

(123) Bender, R.; Salaita, K. Molecular Force Sensors. *ACS* **2022**.

(124) Li, H.; Zhang, C.; Hu, Y.; Liu, P.; Sun, F.; Chen, W.; Zhang, X.; Ma, J.; Wang, W.; Wang, L.; Wu, P.; Liu, Z. A Reversible Shearing DNA Probe for Visualizing Mechanically Strong Receptors in Living Cells. *Nat. Cell Biol.* **2021**, *23* (6), 642−651.

(125) Brockman, J. M.; Blanchard, A. T.; Pui-Yan, V.; Derricotte, W. D.; Zhang, Y.; Fay, M. E.; Lam, W. A.; Evangelista, F. A.; Mattheyses, A. L.; Salaita, K. Mapping the 3D Orientation of Piconewton Integrin Traction Forces. *Nat. Methods* **2018**, *15* (2), 115−118.

(126) Vorselen, D.; Wang, Y.; de Jesus, M. M.; Shah, P. K.; Footer, M. J.; Huse, M.; Cai, W.; Theriot, J. A. Microparticle Traction Force

Microscopy Reveals Subcellular Force Exertion Patterns in Immune Cell-Target Interactions. *Nat. Commun.* **2020**, *11* (1), 1.

(127) Ma, R.; Kellner, A. V.; Ma, V. P. Y.; Su, H.; Deal, B. R.; Brockman, J. M.; Salaita, K. DNA Probes That Store Mechanical Information Reveal Transient Piconewton Forces Applied by T Cells. *Proc. Natl. Acad. Sci. U. S. A.* **2019**, *116* (34), 16949−16954.

(128) Feng, Y.; Zhao, X.; White, A. K.; Garcia, K. C.; Fordyce, P. M. A Bead-Based Method for High-Throughput Mapping of the Sequence- and Force-Dependence of T Cell Activation. *Nat. Methods* **2022**, *19* (10), 1295−1305.

(129) Hickey, J. W.; Dong, Y.; Chung, J. W.; Salathe, S. F.; Pruitt, H. C.; Li, X.; Chang, C.; Fraser, A. K.; Bessell, C. A.; Ewald, A. J.; Gerecht, S.; Mao, H. Q.; Schneck, J. P. Engineering an Artificial T-Cell Stimulating Matrix for Immunotherapy. *Adv. Mater.* **2019**, *31* (23), 1.

(130) Kenneth, S. B., Ed., *Microscale Diagnostic Techniques*; Springer-Verlag, 2005.

(131) Furst, E. M.; Squires, T. M. *Microrheology*; Oxford University Press, 2018. .

(132) Xing, Z.; Caciagli, A.; Cao, T.; Stoev, I.; Zupkauskas, M.; O'Neill, T.; Wenzel, T.; Lamboll, R.; Liu, D.; Eiser, E. Microrheology of DNA Hydrogels. *Proc. Natl. Acad. Sci. U. S. A.* **2018**, *115* (32), 8137−8142.

(133) Keller, M.; Tharmann, R.; Dichtl, M. A.; Bausch, A. R.; Sackmann, E. Slow Filament Dynamics and Viscoelasticity in Entangled and Active Act in Networks. *Philosophical Transactions of the Royal Society A: Mathematical, Physical and Engineering Sciences* **2003**, *361*, 699−712.

(134) Hosu, B. G.; Jakab, K.; Bánki, P.; Tóth, F. I.; Forgacs, G. Magnetic Tweezers for Intracellular Applications. *Rev. Sci. Instrum.* **2003**, *74* (9), 4158−4163.

(135) Bausch, A. R.; Möller, W.; Sackmann, E. Measurement of Local Viscoelasticity and Forces in Living Cells by Magnetic Tweezers. *Biophys. J.* **1999**, *76* (1), 573−579.

(136) Bausch, A. R.; Hellerer, U.; Essler, M.; Aepfelbacher, M.; Sackmann, E. Rapid Stiffening of Integrin Receptor-Actin Linkages in Endothelial Cells Stimulated with Thrombin: A Magnetic Bead Microrheology Study. *Biophys. J.* **2001**, *80* (6), 2649−2657.

(137) Feneberg, W.; Westphal, M.; Sackmann, E. Dictyostelium Cells' Cytoplasm as an Active Viscoplastic Body. *Eur. Biophys. J.* **2001**, *30* (4), 284−294.

(138) Pokki, J.; Zisi, I.; Schulman, E.; Indana, D.; Chaudhuri, O. Magnetic Probe-Based Microrheology Reveals Local Softening and Stiffening of 3D Collagen Matrices by Fibroblasts. *Biomed Microdevices* **2021**, *23* (2), 1.

(139) Kong, D.; Peng, L.; Bosch-Fortea, M.; Chrysanthou, A.; Alexis, C. V. J. M.; Matellan, C.; Zarbakhsh, A.; Mastroianni, G.; del Rio Hernandez, A.; Gautrot, J. E. Impact of the Multiscale Viscoelasticity of Quasi-2D Self-Assembled Protein Networks on Stem Cell Expansion at Liquid Interfaces. *Biomaterials* **2022**, *284*, 121494.

(140) Ashkin, A. ACCELERATION AND TRAPPING OF PARTICLES BY RADIATION PRESSURE. *PHYSICAL REVIEW LETTERS* **1970**, *24*, 156−159.

(141) Meng, L.; Cai, F.; Li, F.; Zhou, W.; Niu, L.; Zheng, H. Acoustic Tweezers. *Journal of Physics D: Applied Physics* **2019**, *52*, 273001.

(142) Marzo, A.; Drinkwater, B. W. Holographic Acoustic Tweezers. *Proc. Natl. Acad. Sci. U. S. A.* **2019**, *116* (1), 84−89.

(143) Sitters, G.; Kamsma, D.; Thalhammer, G.; Ritsch-Marte, M.; Peterman, E. J. G.; Wuite, G. J. L. Acoustic Force Spectroscopy. *Nat. Methods* **2015**, *12* (1), 47−50.

(144) Ozcelik, A.; Rufo, J.; Guo, F.; Gu, Y.; Li, P.; Lata, J.; Huang, T. J. Acoustic Tweezers for the Life Sciences. *Nature Methods* **2018**, *15*, 1021−1028.

(145) Polychronopoulos, S.; Memoli, G. Acoustic Levitation with Optimized Reflective Metamaterials. *Sci. Rep* **2020**, *10* (1), 1.

(146) Guo, F.; Mao, Z.; Chen, Y.; Xie, Z.; Lata, J. P.; Li, P.; Ren, L.; Liu, J.; Yang, J.; Dao, M.; Suresh, S.; Huang, T. J. Three-Dimensional

Manipulation of Single Cells Using Surface Acoustic Waves. *Proc. Natl. Acad. Sci. U. S. A.* **2016**, *113* (6), 1522−1527.

(147) Hwang, J. Y.; Yoon, C. W.; Lim, H. G.; Park, J. M.; Yoon, S.; Lee, J.; Shung, K. K. Acoustic Tweezers for Studying Intracellular Calcium Signaling in SKBR-3 Human Breast Cancer Cells. *Ultrasonics* **2015**, *63*, 94−101.

(148) Liu, H. C.; Gang, E. J.; Kim, H. N.; Lim, H. G.; Jung, H.; Chen, R.; Abdel-Azim, H.; Shung, K. K.; Kim, Y. M. Characterizing Deformability of Drug Resistant Patient-Derived Acute Lympho-blastic Leukemia (ALL) Cells Using Acoustic Tweezers. *Sci. Rep* **2018**, *8* (1), 1.

(149) Lim, H. G.; Liu, H. C.; Yoon, C. W.; Jung, H.; Kim, M. G.; Yoon, C.; Kim, H. H.; Shung, K. K. Investigation of Cell Mechanics Using Single-Beam Acoustic Tweezers as a Versatile Tool for the Diagnosis and Treatment of Highly Invasive Breast Cancer Cell Lines: An in Vitro Study. *Microsyst Nanoeng* **2020**, *6* (1), 1.

(150) Snoj, Ž.; Wu, C. H.; Taljanovic, M. S.; Dumić-Čule, I.; Drakonaki, E. E.; Klauser, A. S. Ultrasound Elastography in Musculoskeletal Radiology: Past, Present, and Future. *Semin Musculoskelet Radiol* **2020**, *24* (2), 156−166.

(151) Caenen, A.; Bezy, S.; Pernot, M.; Nightingale, K. R.; Vos, H. J.; Voigt, J.-U.; Segers, P.; D'hooge, J. Ultrasound Shear Wave Elastography in Cardiology. *JACC Cardiovasc. Imaging* **2024**, *17*, 314−329.

(152) Dirk-André Clevert; Mirko D'Onofrio; Emilio Quaia; *Atlas of Elastosonography*; Springer International Publishing, 2017. .

(153) Prado-Costa, R.; Rebelo, J.; Monteiro-Barroso, J.; Preto, A. S. Ultrasound Elastography: Compression Elastography and Shear-Wave Elastography in the Assessment of Tendon Injury. *Insights into Imaging* **2018**, *9*, 791−814.

(154) Ozturk, A.; Grajo, J. R.; Dhyani, M.; Anthony, B. W.; Samir, A. E. Principles of Ultrasound Elastography. *Abdominal Radiology* **2018**, *43* (4), 773−785.

(155) Wee, T. C.; Simon, N. G. Ultrasound Elastography for the Evaluation of Peripheral Nerves: A Systematic Review. *Muscle and Nerve* **2019**, *60*, 501−512.

(156) Li, G.-Y.; Cao, Y. Mechanics of Ultrasound Elastography. *Proceedings of the Royal Society A: Mathematical, Physical and Engineering Sciences* **2017**, *473*, 20160841.

(157) Sigrist, R. M. S.; Liau, J.; Kaffas, A. El; Chammas, M. C.; Willmann, J. K. Ultrasound Elastography: Review of Techniques and Clinical Applications. *Theranostics* **2017**, *7*, 1303−1329.

(158) Barr, R. G.; Nakashima, K.; Amy, D.; Cosgrove, D.; Farrokh, A.; Schafer, F.; Bamber, J. C.; Castera, L.; Choi, B. I.; Chou, Y. H.; Dietrich, C. F.; Ding, H.; Ferraioli, G.; Filice, C.; Friedrich-Rust, M.; Hall, T. J.; Nightingale, K. R.; Palmeri, M. L.; Shiina, T.; Suzuki, S.; Sporea, I.; Wilson, S.; Kudo, M. WFUMB Guidelines and Recommendations for Clinical Use of Ultrasound Elastography: Part 2: Breast. *Ultrasound Med. Biol.* **2015**, *41* (5), 1148−1160.

(159) Ferraioli, G.; Filice, C.; Castera, L.; Choi, B. I.; Sporea, I.; Wilson, S. R.; Cosgrove, D.; Dietrich, C. F.; Amy, D.; Bamber, J. C.; Barr, R.; Chou, Y. H.; Ding, H.; Farrokh, A.; Friedrich-Rust, M.; Hall, T. J.; Nakashima, K.; Nightingale, K. R.; Palmeri, M. L.; Schafer, F.; Shiina, T.; Suzuki, S.; Kudo, M. WFUMB Guidelines and Recommendations for Clinical Use of Ultrasound Elastography: Part 3: Liver. *Ultrasound Med. Biol.* **2015**, *41* (5), 1161−1179.

(160) Barr, R. G.; Cosgrove, D.; Brock, M.; Cantisani, V.; Correas, J. M.; Postema, A. W.; Salomon, G.; Tsutsumi, M.; Xu, H. X.; Dietrich, C. F. WFUMB Guidelines and Recommendations on the Clinical Use of Ultrasound Elastography: Part 5. Prostate. *Ultrasound in Medicine and Biology* **2017**, *43*, 27−48.

(161) Cosgrove, D.; Barr, R.; Bojunga, J.; Cantisani, V.; Chammas, M. C.; Dighe, M.; Vinayak, S.; Xu, J. M.; Dietrich, C. F. WFUMB Guidelines and Recommendations on the Clinical Use of Ultrasound Elastography: Part 4. Thyroid. *Ultrasound in Medicine and Biology* **2017**, *43*, 4−26.

(162) Shiina, T.; Nightingale, K. R.; Palmeri, M. L.; Hall, T. J.; Bamber, J. C.; Barr, R. G.; Castera, L.; Choi, B. I.; Chou, Y. H.; Cosgrove, D.; Dietrich, C. F.; Ding, H.; Amy, D.; Farrokh, A.;

Ferraioli, G.; Filice, C.; Friedrich-Rust, M.; Nakashima, K.; Schafer, F.; Sporea, I.; Suzuki, S.; Wilson, S.; Kudo, M. WFUMB Guidelines and Recommendations for Clinical Use of Ultrasound Elastography: Part 1: Basic Principles and Terminology. *Ultrasound Med. Biol.* **2015**, *41* (5), 1126−1147.

(163) Jeong, W. K.; Lim, H. K.; Lee, H. K.; Jo, J. M.; Kim, Y. Principles and Clinical Application of Ultrasound Elastography for Diffuse Liver Disease. *Ultrasonography* **2014**, *33*, 149−160.

(164) Ponnekanti, H.; Ophir, J.; Huang, Y.; Céspedes, I. Fundamental Mechanical Limitations on the Visualization of Elasticity Contrast in Elastography. *Ultrasound Med. Biol.* **1995**, *21* (4), 533−543.

(165) Bruce, M.; Kolokythas, O.; Ferraioli, G.; Filice, C.; O'Donnell, M. Limitations and Artifacts in Shear-Wave Elastography of the Liver. *Biomed Eng. Lett.* **2017**, *7* (2), 81−89.

(166) Franchi-Abella, S.; Elie, C.; Correas, J.-M. Ultrasound Elastography: Advantages, Limitations and Artefacts of the Different Techniques from a Study on a Phantom. *Diagn Interv Imaging* **2013**, *94* (5), 497−501.

(167) Li, R.; Qian, X.; Gong, C.; Zhang, J.; Liu, Y.; Xu, B.; Humayun, M. S.; Zhou, Q. Simultaneous Assessment of the Whole Eye Biomechanics Using Ultrasonic Elastography. *IEEE Trans. Biomed. Eng.* **2023**, *70*, 1310−1317.

(168) Prager, J.; Adams, C. F; Delaney, A. M; Chanoit, G.; Tarlton, J. F; Wong, L.-F.; Chari, D. M; Granger, N. Stiffness-matched biomaterial implants for cell delivery: clinical, intraoperative ultrasound elastography provides a "target" stiffness for hydrogel synthesis in spinal cord injury. *J. Tissue Eng.* **2020**, *11*, 2041731420934480.

(169) Liu, H. C.; Gang, E. J.; Kim, H. N.; Lim, H. G.; Jung, H.; Chen, R.; Abdel-Azim, H.; Shung, K. K.; Kim, Y. M. Characterizing Deformability of Drug Resistant Patient-Derived Acute Lympho-blastic Leukemia (ALL) Cells Using Acoustic Tweezers. *Sci. Rep* **2018**, *8* (1), 1.

(170) Gasik, M.; Zühlke, A.; Haaparanta, A. M.; Muhonen, V.; Laine, K.; Bilotsky, Y.; Kellomäki, M.; Kiviranta, I. The Importance of Controlled Mismatch of Biomechanical Compliances of Implantable Scaffolds and Native Tissue for Articular Cartilage Regeneration. *Front Bioeng Biotechnol* **2018**, *6* (NOV), 187.

(171) Hendriks, J. A. A.; Moroni, L.; Riesle, J.; de Wijn, J. R.; van Blitterswijk, C. A. The Effect of Scaffold-Cell Entrapment Capacity and Physico-Chemical Properties on Cartilage Regeneration. *Biomaterials* **2013**, *34* (17), 4259−4265.

(172) Şenol, M. S.; Özer, H. Architecture of Cartilage Tissue and Its Adaptation to Pathological Conditions. *Comparative Kinesiology of the Human Body: Normal and Pathological Conditions* **2020**, 91−100.

(173) Grad, S.; Loparic, M.; Peter, R.; Stolz, M.; Aebi, U.; Alini, M. Sliding Motion Modulates Stiffness and Friction Coefficient at the Surface of Tissue Engineered Cartilage. *Osteoarthritis Cartilage* **2012**, *20* (4), 288−295.

(174) Lee, H. P.; Gu, L.; Mooney, D. J.; Levenston, M. E.; Chaudhuri, O. Mechanical Confinement Regulates Cartilage Matrix Formation by Chondrocytes. *Nature Materials 2017 16:12* **2017**, *16* (12), 1243−1251.

(175) Lee, H. J.; Seo, Y.; Kim, H. S.; Lee, J. W.; Lee, K. Y. Regulation of the Viscoelastic Properties of Hyaluronate-Alginate Hybrid Hydrogel as an Injectable for Chondrocyte Delivery. *ACS Omega* **2020**, *5* (25), 15567−15575.

(176) Zhang, W.; Liu, Y.; Kassab, G. S. Viscoelasticity Reduces the Dynamic Stresses and Strains in the Vessel Wall: Implications for Vessel Fatigue. *Am. J. Physiol Heart Circ Physiol* **2007**, *293* (4), H2355.

(177) Pashneh-Tala, S.; MacNeil, S.; Claeyssens, F. The Tissue-Engineered Vascular Graft—Past, Present, and Future. *Tissue Eng. Part B Rev.* **2016**, *22* (1), 68.

(178) Walden, R.; L'italien, G. J.; Megerman, J.; Abbott, W. M. Matched Elastic Properties and Successful Arterial Grafting. *Archives of Surgery* **1980**, *115* (10), 1166−1169.

(179) Abbott, W. M.; Megerman, J.; Hasson, J. E.; L'Italien, G.; Warnock, D. F. Effect of Compliance Mismatch on Vascular Graft Patency. *J. Vasc Surg* **1987**, 5 (2), 376−382.

(180) Dahl, S. L. M.; Kypson, A. P.; Lawson, J. H.; Blum, J. L.; Strader, J. T.; Li, Y.; Manson, R. J.; Tente, W. E.; DiBernardo, L.; Hensley, M. T.; Carter, R.; Williams, T. P.; Prichard, H. L.; Dey, M. S.; Begelman, K. G.; Niklason, L. E. Readily Available Tissue-Engineered Vascular Grafts. *Sci. Transl Med.* **2011**, 3 (68), 1.

(181) Camasão, D. B.; Mantovani, D. The Mechanical Characterization of Blood Vessels and Their Substitutes in the Continuous Quest for Physiological-Relevant Performances. A Critical Review. *Mater. Today Bio* **2021**, 10, 100106.

(182) Hinton, R. B.; Yutzey, K. E. Heart Valve Structure and Function in Development and Disease. *Annual Review of Physiology,* **2011**, 73, 29−46.

(183) Constable, M.; Burton, H. E.; Lawless, B. M.; Gramigna, V.; Buchan, K. G.; Espino, D. M. Effect of Glutaraldehyde Based Cross-Linking on the Viscoelasticity of Mitral Valve Basal Chordae Tendineae. *Biomed Eng. Online* **2018**, 17 (1), 1−14.

(184) Baxter, J.; Buchan, K. G.; Espino, D. M. Viscoelastic Properties of Mitral Valve Leaflets: An Analysis of Regional Variation and Frequency-Dependency. *Journal of Engineering in Medicine, Sage* **2017**, 231 (10), 938−944.

(185) Anssari-Benam, A.; Bucchi, A.; Screen, H. R. C.; Evans, S. L. A Transverse Isotropic Viscoelastic Constitutive Model for Aortic Valve Tissue. *R Soc. Open Sci.* **2017**, 4 (1), 160585.

(186) Shemesh, M.; Asher, R.; Zylberberg, E.; Guilak, F.; Linder-Ganz, E.; Elsner, J. J. Viscoelastic Properties of a Synthetic Meniscus Implant. *J. Mech Behav Biomed Mater.* **2014**, 29, 42−55.

(187) Carnicer-Lombarte, A.; Barone, D. G.; Dimov, I. B.; Hamilton, R. S.; Prater, M.; Zhao, X.; Rutz, A. L.; Malliaras, G. G.; Lacour, S. P.; Bryant, C. E.; Fawcett, J. W.; Franze, K.Foreign Body Reaction Is Triggered in Vivo by Cellular Mechanosensing of Implants Stiffer than Host Tissue. *bioRxiv*, 2022, p 829648

(188) Wei, Z.; Schnellmann, R.; Pruitt, H. C.; Gerecht, S. Hydrogel Network Dynamics Regulate Vascular Morphogenesis. *Cell Stem Cell* **2020**, 27 (5), 798−812.

(189) Chaudhuri, O.; Gu, L.; Klumpers, D.; Darnell, M.; Bencherif, S. A.; Weaver, J. C.; Huebsch, N.; Lee, H. P.; Lippens, E.; Duda, G. N.; Mooney, D. J. Hydrogels with Tunable Stress Relaxation Regulate Stem Cell Fate and Activity. *Nature Materials 2015 15:3* **2016**, 15 (3), 326−334.

(190) Zhao, X.; Huebsch, N.; Mooney, D. J.; Suo, Z. Stress-Relaxation Behavior in Gels with Ionic and Covalent Crosslinks. *J. Appl. Phys.* **2010**, 107 (6), 1.

(191) Elosegui-Artola, A.; Gupta, A.; Najibi, A. J.; Seo, B. R.; Garry, R.; Tringides, C. M.; de Lázaro, I.; Darnell, M.; Gu, W.; Zhou, Q.; Weitz, D. A.; Mahadevan, L.; Mooney, D. J. Matrix Viscoelasticity Controls Spatiotemporal Tissue Organization. *Nature Materials 2022 22:1* **2023**, 22 (1), 117−127.

(192) Wang, L. L.; Highley, C. B.; Yeh, Y. C.; Galarraga, J. H.; Uman, S.; Burdick, J. A. Three-Dimensional Extrusion Bioprinting of Single- and Double-Network Hydrogels Containing Dynamic Covalent Crosslinks. *J. Biomed Mater. Res. A* **2018**, 106 (4), 865−875.

(193) Gungor-Ozkerim, P. S.; Inci, I.; Zhang, Y. S.; Khademhosseini, A.; Dokmeci, M. R. Bioinks for 3D Bioprinting: An Overview. *Biomater Sci.* **2018**, 6 (5), 915−946.

(194) Nam, K. H.; Smith, A. S. T.; Lone, S.; Kwon, S.; Kim, D. H. Biomimetic 3D Tissue Models for Advanced High-Throughput Drug Screening. *SLAS Technol.* **2015**, 20 (3), 201−215.

(195) Murphy, M. C.; Huston, J.; Ehman, R. L. MR Elastography of the Brain and Its Application in Neurological Diseases. *Neuroimage* **2019**, 187, 176−183.

(196) Streitberger, K. J.; Sack, I.; Krefting, D.; Pfüller, C.; Braun, J.; Paul, F.; Wuerfel, J. Brain Viscoelasticity Alteration in Chronic-Progressive Multiple Sclerosis. *PLoS One* **2012**, 7 (1), No. e29888.

(197) Feng, Y.; Murphy, M. C.; Hojo, E.; Li, F.; Roberts, N. Magnetic Resonance Elastography in the Study of Neurodegenerative Diseases. *J. Magn. Reson. Imaging JMRI* **2024**, 59, 82−96.

(198) Mierke, C. T. Viscoelasticity Acts as a Marker for Tumor Extracellular Matrix Characteristics. *Front Cell Dev Biol.* **2021**, 9, 3536.

(199) Taubenberger, A. V.; Girardo, S.; Träber, N.; Fischer-Friedrich, E.; Kräter, M.; Wagner, K.; Kurth, T.; Richter, I.; Haller, B.; Binner, M.; Hahn, D.; Freudenberg, U.; Werner, C.; Guck, J. 3D Microenvironment Stiffness Regulates Tumor Spheroid Growth and Mechanics via P21 and ROCK. *Adv. Biosyst* **2019**, 3 (9), 1900128.

(200) Grigoryan, B.; Paulsen, S. J.; Corbett, D. C.; Sazer, D. W.; Fortin, C. L.; Zaita, A. J.; Greenfield, P. T.; Calafat, N. J.; Gounley, J. P.; Ta, A. H.; Johansson, F.; Randles, A.; Rosenkrantz, J. E.; Louis-Rosenberg, J. D.; Galie, P. A.; Stevens, K. R.; Miller, J. S. Multivascular Networks and Functional Intravascular Topologies within Biocompatible Hydrogels. *Science (1979)* **2019**, 364 (6439), 458−464.

(201) Fang, J. Y.; Tan, S.-J.; Yang, Z.; Tayag, C.; Han, B. Tumor Bioengineering Using a Transglutaminase Crosslinked Hydrogel. *PLoS One* **2014**, 9 (8), e105616.

(202) Pradhan, S.; Slater, J. H. Tunable Hydrogels for Controlling Phenotypic Cancer Cell States to Model Breast Cancer Dormancy and Reactivation. *Biomaterials* **2019**, 215, 119177.

(203) Fenner, J.; Stacer, A. C.; Winterroth, F.; Johnson, T. D.; Luker, K. E.; Luker, G. D. Macroscopic Stiffness of Breast Tumors Predicts Metastasis. *Sci. Rep* **2014**, 4, 1−8.

(204) Stowers, R. S.; Shcherbina, A.; Israeli, J.; Gruber, J. J.; Chang, J.; Nam, S.; Rabiee, A.; Teruel, M. N.; Snyder, M. P.; Kundaje, A.; Chaudhuri, O. Matrix Stiffness Induces a Tumorigenic Phenotype in Mammary Epithelium through Changes in Chromatin Accessibility. *Nat. Biomed Eng.* **2019**, 3 (12), 1009−1019.

(205) Reid, S. E.; Kay, E. J.; Neilson, L. J.; Henze, A.; Serneels, J.; McGhee, E. J.; Dhayade, S.; Nixon, C.; Mackey, J. B.; Santi, A.; Swaminathan, K.; Athineos, D.; Papalazarou, V.; Patella, F.; Román-Fernández, A.; ElMaghloob, Y.; Hernandez-Fernaud, J. R.; Adams, R. H.; Ismail, S.; Bryant, D. M.; Salmeron-Sanchez, M.; Machesky, L. M.; Carlin, L. M.; Blyth, K.; Mazzone, M.; Zanivan, S. Tumor Matrix Stiffness Promotes Metastatic Cancer Cell Interaction with the Endothelium. *EMBO J.* **2017**, 36 (16), 2373−2389.

(206) Watson, A. W.; Grant, A. D.; Parker, S. S.; Hill, S.; Whalen, M. B.; Chakrabarti, J.; Harman, M. W.; Roman, M. R.; Forte, B. L.; Gowan, C. C.; Castro-Portuguez, R.; Stolze, L. K.; Franck, C.; Cusanovich, D. A.; Zavros, Y.; Padi, M.; Romanoski, C. E.; Mouneimne, G. Breast Tumor Stiffness Instructs Bone Metastasis via Maintenance of Mechanical Conditioning. *Cell Rep* **2021**, 35 (13), 109293.

(207) Leung, C. M.; de Haan, P.; Ronaldson-Bouchard, K.; Kim, G. A.; Ko, J.; Rho, H. S.; Chen, Z.; Habibovic, P.; Jeon, N. L.; Takayama, S.; Shuler, M. L.; Vunjak-Novakovic, G.; Frey, O.; Verpoorte, E.; Toh, Y. C. A Guide to the Organ-on-a-Chip. *Nature Reviews Methods Primers* **2022**, 1.

(208) Low, L. A.; Mummery, C.; Berridge, B. R.; Austin, C. P.; Tagle, D. A. Organs-on-Chips: Into the next Decade. *Nature Reviews Drug Discovery* **2021**, 20, 345−361.

(209) Ingber, D. E. Human Organs-on-Chips for Disease Modelling, Drug Development and Personalized Medicine. *Nature Reviews Genetics* **2022**, 23, 467−491.

(210) Malik, M.; Yang, Y.; Fathi, P.; Mahler, G. J.; Esch, M. B. Critical Considerations for the Design of Multi-Organ Microphysiological Systems (MPS). *Frontiers in Cell and Developmental Biology* **2021**, 9, 1.

(211) Fan, H.; Demirci, U.; Chen, P. Emerging Organoid Models: Leaping Forward in Cancer Research. *J. Hematol Oncol* **2019**, 12 (1), 1−10.

(212) Weber, C. Organoids Test Drug Response. *Nat. Cell Biol.* **2018**, 20 (6), 634.

(213) Tatullo, M.; Marrelli, B.; Benincasa, C.; Aiello, E.; Makeeva, I.; Zavan, B.; Ballini, A.; De Vito, D.; Spagnuolo, G. Organoids in Translational Oncology. *Journal of Clinical Medicine* **2020**, 9, 1−16.

(214) Zhang, Z.; Arshad, M.; Bertin, V.; Almohamad, S.; Raphael, E.; Salez, T.; Maali, A. Contactless Rheology of Soft Gels Over a Broad Frequency Range. *Phys. Rev. Appl.* **2022**, 17, 064045.

(215) Muntz, I.; Richards, J. A.; Brown, S.; Schofield, A. B.; Rey, M.; Thijssen, J. H. J. Contactless interfacial rheology: Probing shear at liquid-liquid interfaces without an interfacial geometry via fluorescence microscopy. *J. Rheol.* **2023**, *67*, 67−80.

(216) Prakadan, S. M.; Shalek, A. K.; Weitz, D. A. Scaling by Shrinking: Empowering Single-Cell "omics" with Microfluidic Devices. *Nature Reviews Genetics* **2017**, *18*, 345−361.

(217) Rigato, A.; Miyagi, A.; Scheuring, S.; Rico, F. High-Frequency Microrheology Reveals Cytoskeleton Dynamics in Living Cells. *Nat. Phys.* **2017**, *13* (8), 771−775.